

การเปิดวงอ็อกไซค์เร่งปฏิกิริยาด้วยไอรอนออกไซค์ฟิลลาร์เคลย์



นางสาวปิยรัตน์ ตรีกิตติวงศ์

สถาบันวิทยบริการ
จุฬาลงกรณ์มหาวิทยาลัย

วิทยานิพนธ์นี้เป็นส่วนหนึ่งของการศึกษาตามหลักสูตรปริญญาวิทยาศาสตรมหาบัณฑิต

สาขาวิชาปิโตรเคมี และวิทยาศาสตร์พอลิเมอร์

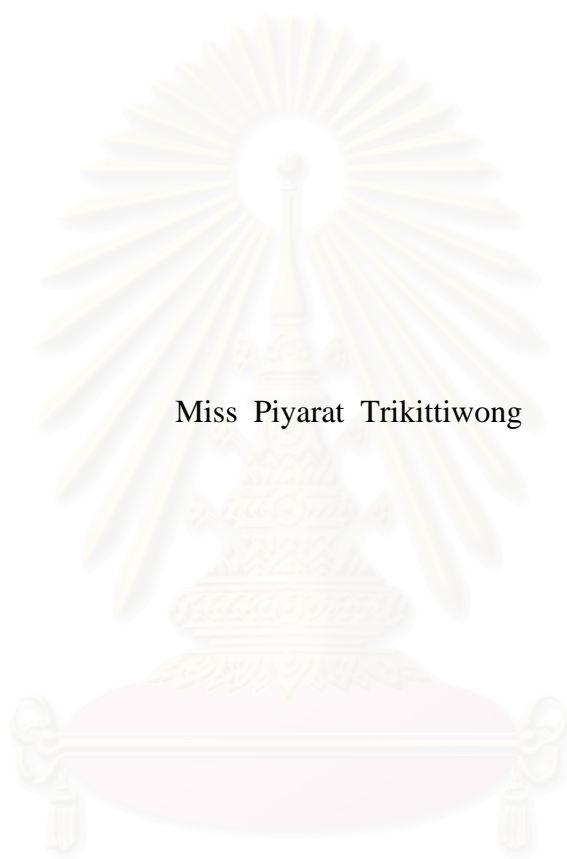
คณะวิทยาศาสตร์ จุฬาลงกรณ์มหาวิทยาลัย

ปีการศึกษา 2548

ISBN 974-14-1994-5

ลิขสิทธิ์ของจุฬาลงกรณ์มหาวิทยาลัย

EPOXIDE RING OPENING CATALYZED BY IRON OXIDE-PILLARED CLAY



Miss Piyarat Trikittiwong

สถาบันวิทยบริการ
จุฬาลงกรณ์มหาวิทยาลัย

A Thesis Submitted in Partial Fulfillment of the Requirements
for the Degree of Master of Science Program in Petrochemistry and Polymer Science

Faculty of Science

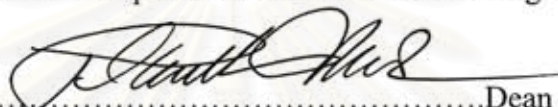
Chulalongkorn University

Academic Year 2005

ISBN 974-14-1994-5


Thesis Title EPOXIDE RING OPENING CATALYZED BY IRON
OXIDE-PILLARED CLAY
By Miss Piyarat Trikittiwong
Field of Study Petrochemistry and Polymer Science
Thesis Advisor Nipaka Sukpirom, Ph.D.
Thesis Co-Advisor Assistant Professor Warinthorn Chavasiri, Ph.D.

Accepted by the Faculty of Science, Chulalongkorn University in
Partial Fulfillment of the Requirements for the Master's Degree



.....Dean of the Faculty of Science
(Professor Piemsak Menasveta, Ph.D.)

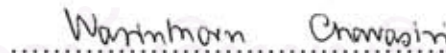
Thesis Committee



.....Chairman
(Associate Professor Supawan Tantayanon, Ph.D.)



..... Thesis Advisor
(Nipaka Sukpirom, Ph.D.)



.....Thesis Co-Advisor
(Assistant Professor Warinthorn Chavasiri, Ph.D.)



.....Member
(Associate Professor Wimonrat Trakarnpruk, Ph.D.)



.....Member
(Associate Professor Vithaya Ruangpornvisuti, Ph.D.)

ปิยรัตน์ ตรีภักดีวงศ์ : การเปิดวงอีพอกไซด์เร่งปฏิกิริยาด้วยไอรอนออกไซด์ฟิลลาร์เคลย์ (EPOXIDE RING OPENING CATALYZED BY IRON OXIDE-PILLARED CLAY) อ. ที่ปรึกษา: ดร. นิปกา สุขภิรมย์, อ. ที่ปรึกษาร่วม: ผศ.ดร.วรินทร์ ชวศิริ, 82 หน้า, ISBN 974-14-1994-5

ไอรอนออกไซด์ฟิลลาร์เคลย์ เช่น ไอรอนฟิลลาร์เฮกโทไรด์ และไอรอนฟิลลาร์เบนโทไนด์ สังเคราะห์ได้โดยการสอดแทรกสารประกอบเหล็กเข้าไปในระหว่างชั้นของเคลย์ แล้วนำไปเผาที่ อุณหภูมิ 300°C เป็นเวลา 5 ชั่วโมง พิสฐานโครงสร้างของผลิตภัณฑ์ที่สังเคราะห์ได้ด้วยเทคนิค การเลี้ยวเบนของรังสีเอ็กซ์ การดูดซับแก๊สไนโตรเจน ริดอกซ์ไทเทรชันและเบสไทเทรชัน ไอรอนฟิลลาร์เฮกโทไรด์และไอรอนฟิลลาร์เบนโทไนด์ที่ได้จากการสังเคราะห์ แสดงโครงสร้างแบบโพรง ขนาดกลาง ที่ประกอบด้วยไอรอน 21.01% และ 29.18% โดยน้ำหนัก ตามลำดับ ตัวเร่งปฏิกิริยาที่ สังเคราะห์ได้ นำไปใช้สำหรับปฏิกิริยาการเปิดวงสไตรีนออกไซด์ด้วยเมทานอล เปรียบเทียบ กับเคลย์บริสุทธิ์และไอรอนออกไซด์ ได้ผลิตภัณฑ์ 2-เมทอกซี-2-เฟนิลเอทานอล ในปริมาณสูงเมื่อ ใช้ไอรอนฟิลลาร์เบนโทไนด์ในปริมาณร้อยละ 30 ค่อน้ำหนักของสารตั้งต้น โดยทำปฏิกิริยาที่ อุณหภูมิ 70°C และใช้เวลาทำปฏิกิริยา 10 นาที ปฏิกิริยานี้เกิดขึ้นได้อย่างรวดเร็วภายใต้ภาวะที่ไม่ รุนแรง โดยภาวะที่เหมาะสมสำหรับการเปิดวง สามารถนำไปใช้กับอีพอกไซด์ชนิดอื่น ๆ ดังเช่น 1-โคเดซินออกไซด์ ไซโคลเฮกซินออกไซด์ บิวทิลไกลซิซิลอีเทอร์ เทอร์เทียรบิวทิลไกลซิซิล อีเทอร์ และ แอลฟาไพเนนออกไซด์ พบว่าได้ปริมาณผลิตภัณฑ์ที่ต้องการในระดับปานกลางถึงสูง

สถาบันวิทยบริการ จุฬาลงกรณ์มหาวิทยาลัย

สาขาวิชา ปิโตรเคมีและวิทยาศาสตร์พอลิเมอร์ ลายมือชื่อนิสิต ปิยรัตน์ ตรีภักดีวงศ์
ปีการศึกษา 2548 ลายมือชื่ออาจารย์ที่ปรึกษา ผศ.ดร.วรินทร์ ชวศิริ
ลายมือชื่ออาจารย์ที่ปรึกษาร่วม ผศ.ดร.วรินทร์ ชวศิริ

4772376623: MAJOR PETROCHEMISTRY AND POLYMER SCIENCE

KEY WORD: RING OPENING / EPOXIDE / PILLARED CLAY

PIYARAT TRIKITTIWONG: EPOXIDE RING OPENING CATALYZED BY IRON OXIDE-PILLARED CLAY. THESIS ADVISOR: NIPAKA SUKPIROM, Ph.D. THESIS CO-ADVISOR: ASST. PROF. WARINTHORN CHAVASIRI, Ph.D., 82 pp. ISBN 974-14-1994-5

Iron oxide pillared clays (Fe-pillared clays) such as Fe-pillared hectorite and Fe-pillared bentonite were synthesized by the intercalation of iron complexes into clay interlayers and calcinations at 300°C for 5 h. The synthesized products were characterized using XRD, N₂ adsorption-desorption, redox and base titration. The synthesized Fe-pillared hectorite and bentonite exhibited the mesoporous structure with iron loading of 21.01 %wt and 29.18 %wt, respectively. The synthesized catalysts were used for styrene oxide ring opening by methanol comparing with pure clays and Fe₂O₃. The quantitative yield of 2-methoxy-2-phenylethanol was obtained using Fe-pillared bentonite in the amount of 30 wt% to styrene oxide, a reaction temperature of 70°C and reaction time of 10 min. This method was carried out in short period of time under mild conditions. The optimized conditions were applied to the ring opening of different epoxides such as 1-dodecene oxide, cyclohexene oxide, butyl glycidyl ether, *tert*-butyl glycidyl ether and α -pinene oxide to furnish the desired products in moderate to excellent yields.

สถาบันวิทยบริการ
จุฬาลงกรณ์มหาวิทยาลัย

Field of Study Petrochemistry and Polymer Science Student's Signature Piyarat Trikittiwong
Academic year 2005 Advisor's Signature Nipaka Sukpirom
Co-advisor's Signature W. Chavasiri

ACKNOWLEDGEMENTS

The success of this thesis can be attributed to the extensive support and assistance from Dr. Nipaka Sukpirom and Assistant Professor Warinthorn Chavasiri, my thesis advisor and thesis co-advisor. I deeply thank them for their valuable advice and guidance in this research and their kindness throughout this study.

I would like to gratitude to Associate Professor Supawan Tantayanon, Associate Professor Wimonrat Trakarnpruk and Associate Professor Vithaya Ruangpornvisuti as the chairman and member of this thesis committee, respectively, for all of their kindness and useful advice in the research.

I would like to gratefully thank VOLCLAY SIAM LIMITED and CERNIC INTERNATIONAL CO., LTD for supporting the clays, hectorite and bentonite. Moreover, I would like to thank Department of Chemistry and Program of Petrochemistry and Polymer Science, Faculty of Science, Chulalongkorn University for the valuable knowledge and experience. I also would like to thank the members of Materials Chemistry and Catalysis Research Unit and Natural Product Research Unit for consideration and generosity.

For all of my friends, I greatly appreciate their help and encouragement throughout the course of my research and study.

Finally, I would like to express my deepest gratitude to my parent for their love, entirely care, understanding and their financial support. The usefulness of this thesis, I dedicate to my father, my mother and all teachers who have taught me since my childhood.

CONTENTS

	Pages
Abstract in Thai.....	iv
Abstract in English.....	v
Acknowledgements.....	vi
List of Figures.....	xii
List of Tables.....	xiii
List of Schemes.....	xiv
List of Abbreviations.....	xv
CHAPTER	
I INTRODUCTION	1
1.1 Literature review on the ring opening of epoxides.....	1
1.1.1 Reaction with homogeneous catalysts.....	1
1.1.2 Reaction with heterogeneous catalysts.....	8
1.2 Literature review on the clay catalysts.....	12
1.3 The goal of this research.....	16
II THEORY	17
2.1 Clay.....	17
2.2 The structure of clay minerals.....	17
2.2.1 Basic units.....	18
2.2.1.1 Tetrahedral sheets.....	18
2.2.1.2 Octahedral sheets.....	18
2.2.2 The combinations of basic sheets divide clays into 2 categories.....	19
2.2.2.1 The 1:1 layered type (T:O).....	19
2.2.2.2 The 2:1 layered type (T:O:T).....	19
2.3 Smectite clay minerals.....	20
2.3.1 Bentonite clay.....	21
2.3.2 Hectorite clay.....	21
2.4 Properties of clay.....	21
2.4.1 Ion exchange.....	21

	Page
2.4.2 Swelling.....	22
2.4.3 Acidity of clays.....	23
2.5 Intercalation.....	23
2.6 Pillaring.....	24
2.7 Pillar clay (PILCs).....	24
2.7.1 Pillaring Agent.....	24
2.8 Characterization of materials.....	25
2.8.1 Powder X-ray diffraction.....	25
2.8.2 Nitrogen adsorption-desorption isotherm.....	26
2.8.3 Determination of iron content in sample.....	28
2.9 Ring-opening of epoxide under acidic conditions.....	29
III EXPERIMENTAL	31
3.1 Instrument, apparatus and analytical measurements.....	31
3.1.1 Centrifuge.....	31
3.1.2 Oven and furnace.....	31
3.1.3 X-ray diffractometer (XRD).....	32
3.1.4 Nitrogen adsorption/desorption (BET).....	32
3.1.6 Gas Chromatography (GC).....	32
3.1.7 Nuclear magnetic resonance spectroscopy (NMR).....	32
3.1.8 Chromatography.....	32
3.2 Starting materials.....	32
3.2.1 Clays.....	32
3.2.2 Chemicals.....	33
3.3 Homoionic clays.....	34
3.3.1 Purification of bentonite.....	34
3.3.2 Na-ion exchange.....	34
3.4 Synthesis of Fe-pillared clays.....	35
3.5 Determination of acidity.....	35
3.6 Determination of iron content by redox titration.....	36
3.7 Preparation of authentic sample.....	37

	Page
3.8 Study on the optimum condition for styrene oxide ring opening reaction.....	39
3.8.1 General procedure.....	39
3.8.2 Effect of the amount of catalyst.....	40
3.8.3 Effect of reaction time and reaction temperature.....	40
3.8.4 Effect of solvent.....	40
3.8.5 Effect of the amount of nucleophile.....	40
3.9 Effect of oxygen nucleophile for styrene oxide ring opening.....	40
3.10 Other epoxides.....	40
3.10.1 1-Dodecene oxide.....	40
3.10.2 Butyl glycidyl ether and <i>tert</i> -butyl glycidyl ether.....	41
3.10.3 Cyclohexene oxide.....	41
3.10.4 α -Pinene oxide.....	41
IV RESULTS AND DISCUSSION.....	42
4.1 The characterization of clays.....	42
4.1.1 X-ray diffraction (XRD).....	42
4.2 The synthesis and characterization of homoionic clays.....	43
4.2.1 Purification of bentonite.....	43
4.2.2 Na-ion exchange.....	44
4.2.2.1 X-ray diffraction of Na-hectorite.....	44
4.2.2.2 X-ray diffraction of Na-bentonite.....	45
4.3 The synthesis and characterization of Fe-pillared clays.....	46
4.3.1 X-ray diffraction of Fe-precursor intercalated clay layer.....	46
4.3.2 X-ray diffraction of Fe-pillared clays.....	47
4.3.3 Determination of iron contents.....	49
4.3.4 Determination of acidity.....	49
4.3.5 Nitrogen adsorption-desorption (Brunauer-Edmelt-Teller method, BET).....	50
4.4 Used catalyst.....	51
4.4.1 X-ray diffraction of used catalyst.....	51

	Page
4.5 Catalytic activity of Fe-pillared clay in epoxide ring opening reaction.....	52
4.5.1 Effect of raw clays (hectorite and bentonite) and Fe-pillared clay catalysts on the reactivity of styrene oxide ring opening...	53
4.5.2 Study on the optimum conditions for styrene oxide ring opening by Fe-pillared hectorite clay.....	54
4.5.2.1 Effect of the reaction time on styrene oxide ring opening reaction.....	54
4.5.2.2 Effect of the amount of catalyst on styrene oxide ring opening reaction.....	55
4.5.3 Study on the optimum conditions for styrene oxide ring opening by Fe-pillared bentonite.....	56
4.5.3.1 Effect of reaction time and reaction temperature for Fe-pillared bentonite catalyzed on styrene oxide ring opening.....	56
4.5.4 Comparism of the effect of Fe-pillared bentonite and Fe-pillared hectorite on styrene oxide ring opening.....	57
4.5.5 Effect of the amount of nucleophile on the styrene oxide ring opening reaction.....	57
4.5.6 Effect of solvent on styrene oxide ring opening reaction.....	58
4.5.6.1 Effect of solvent on the styrene oxide ring opening reaction catalyzed by Fe-pillared bentonite.....	58
4.5.6.2 Effect of solvent and reaction time on the epoxide ring opening reaction catalyzed by Fe-pillared bentonite.....	60
4.5.7 Variation of nucleophile for epoxide ring opening reaction.....	61
4.5.8 The ring opening of other epoxides catalyzed by Fe-pillared bentonite.....	64
4.5.8.1 Ring opening of 1-dodecene oxide.....	64
4.5.8.2 Ring opening of cyclohexene oxide.....	66

	Page
4.5.8.3 Ring opening of butyl glycidyl ether and <i>tert</i> -butyl glycidyl ether.....	67
4.5.8.4 Ring opening of α -pinene oxide.....	69
4.5.9 Summary of the reactivity of various epoxides ring opening catalyzed by Fe-pillared bentonite	71
V CONCLUSION	73
REFERENCES	75
APPENDICES	79
VITA	82



สถาบันวิทยบริการ
จุฬาลงกรณ์มหาวิทยาลัย

LIST OF TABLES

Tables	Pages
2.1 Features of adsorption isotherms.....	27
2.2 IUPAC classification of pores.....	27
3.1 Bentonite and hectorite compositions.....	33
4.1 The iron contents in clays and Fe-pillared clays.....	49
4.2 Acidity values of clays and Fe-pillared clays.....	49
4.3 The BET specific surface area of raw clays and Fe-pillared clays.....	50
4.4 The BET specific surface area of Fe-pillared bentonite and used Fe-pillared bentonite.....	52
4.5 Effect of raw clays (hectorite, bentonite clays) and Fe-pillared clays catalyst on the reactivity of styrene oxide ring opening.....	53
4.6 Effect of the reaction time on styrene oxide ring opening reaction catalyzed by Fe-pillared hectorite.....	54
4.7 Effect of the amount of Fe-pillared hectorite on styrene oxide ring opening reaction.....	55
4.8 Effect of reaction time and reaction temperature on styrene oxide ring opening catalyzed by Fe-pillared bentonite.....	56
4.9 Comparative study on the effect of Fe-pillared hectorite and Fe-pillared bentonite on styrene oxide ring opening.....	57
4.10 Effect of the amount of methanol on the styrene oxide ring opening catalyzed by Fe-pillared bentonite.....	58
4.11 Effect of solvent on styrene oxide ring opening.....	59
4.12 Effect of solvent and reaction time on styrene oxide ring opening reaction catalyzed by Fe-pillared bentonite.....	60
4.13 Variation of oxygen nucleophile in styrene oxide ring opening.....	62
4.14 1-Dodecene oxide ring opening catalyzed by Fe-pillared bentonite.....	64
4.15 Butyl glycidyl ether and <i>tert</i> -butyl glycidyl ether ring opening catalyzed by Fe-pillared bentonite.....	67
4.16 Summary of epoxide ring opening catalyzed by Fe- pillared bentonite.....	71

LIST OF FIGURES

Figures	Pages
2.1 A single tetrahedral silica (a), and a sheet structure (b) of silica tetrahedra arranged in a hexagonal network.....	18
2.2 A single octahedral unit (a), and a sheet structure (b) of octahedral unit arranged in hexagonal network.....	18
2.3 Structure of 1:1 layered type (T = Tetrahedral sheet, O = Octahedral sheet).....	19
2.4 Structure of 2:1 layered type (T = Tetrahedral sheet, O = Octahedral sheet).....	20
2.5 Structure of smectite clay.....	20
2.6 The exchange properties of cations with clays.....	22
2.7 The model of pillared clay structure (cross section).....	24
2.8 Diffraction of X-ray by a regular planes of atoms.....	25
2.9 The IUPAC classification of adsorption isotherm.....	26
4.1 XRD pattern of raw material hectorite.....	42
4.2 XRD pattern of raw material bentonite.....	43
4.3 XRD patterns of raw material bentonite and purified bentonite at centrifugal speed of 4000 rpm.....	44
4.4 XRD patterns of raw material hectorite and Na-hectorite.....	45
4.5 XRD patterns of purified bentonite and Na-bentonite.....	46
4.6 XRD patterns of raw material hectorite and Fe ₁₀ -intercalated hectorite.....	47
4.7 XRD patterns of calcined raw hectorite and HFe ₁₀	48
4.8 XRD patterns of calcined purified bentonite and BFe ₁₀	48
4.9 XRD patterns of BFe ₁₀ and used BFe ₁₀	51

LIST OF SCHEMES

Schemes	Pages
3.1 The heating program used for the calcination of Fe-pillared clays.....	31
4.1 Proposed mechanism of styrene oxide ring opening reaction.....	61
4.2 Proposed mechanism of 1-dodecene oxide ring opening reaction.....	66



สถาบันวิทยบริการ
จุฬาลงกรณ์มหาวิทยาลัย

LIST OF ABBREVIATIONS

BET	Brunauer- Emmett-Teller
δ	chemical shift
J	coupling constant (NMR)
$^{\circ}\text{C}$	degree Celsius
CDCl_3	deuterated chloroform
d	doublet (NMR)
dd	double doublet (NMR)
GC	gas chromatography
g	gram (s)
Hz	hertz
h	hour (s)
MB	mass balance
mL	milliliter (s)
mmol	millimole (s)
mg	milligram (s)
min	minute (s)
M	molar
m	multiplet (NMR)
n	normal
NaOH	sodium hydroxide
NMR	nuclear magnetic resonance
\AA	Angstrom unit
CEC	Cation Exchange Capacity
q	quartet (NMR)
$quin$	quintet (NMR)
rt	room temperature
s	singlet (NMR)
t	triplet (NMR)
XRD	x-ray diffraction

CHAPTER I

INTRODUCTION

The importance of epoxides and products from epoxide ring opening

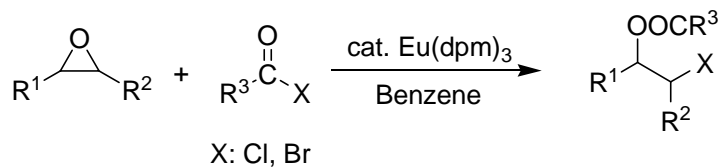
Epoxides are versatile intermediates that serve as prominent building blocks in organic synthesis [1]. The ring of epoxides can be opened under a variety of conditions, although the most practical and widely employed strategy for the synthesis of 1,2-bifunctional compounds is *via* nucleophilic ring opening. The varieties of heteroatom nucleophiles, such as halides, alcohols, amines and thiols are used to convert epoxides to halohydrins, alkoxyalcohols, aminoalcohols and thioalcohols, respectively [2]. The products from epoxide ring opening are indeed important in organic synthesis, pharmaceutical industries [3] and others in chemical fields [4]. For examples β -amino alcohols, typically obtained from opening of epoxides with amines, are versatile intermediates in natural product synthesis [5] and are also used as β -blockers, insecticidal agents and chiral ligands in asymmetric synthesis [6]. β -amino alcohols have become increasingly useful and important in drugs and pharmaceuticals. Chlorohydrins and other halohydrins, obtained from opening of epoxides with TMSCl, are an important class of organic compounds as intermediates in the synthesis of a vast range of biologically active natural and synthetic products, unnatural amino acids, and chiral auxiliaries for asymmetric synthesis [7].

1.1 Literature review on the epoxide ring opening

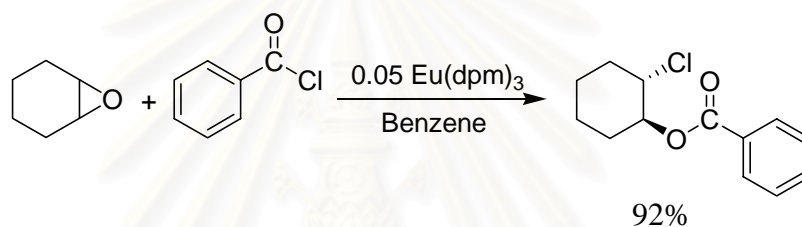
Method of epoxide ring opening

1.1.1 Reactions with homogeneous catalysts

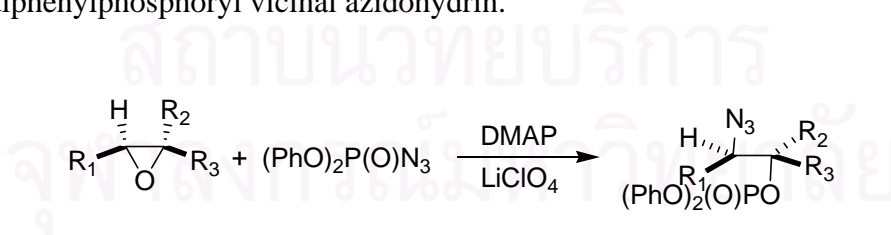
In 1998 Taniguchi and colleagues reported that the lanthanoid complexes catalyze the ring opening reaction of epoxides with acyl halides as a nucleophile to afford the corresponding 2-haloalkyl esters. This communication describes an efficient and a stereoselective synthesis of 2-haloalkyl esters.



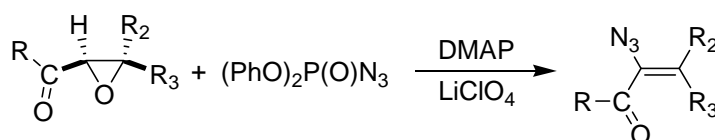
The reaction of cyclohexene oxide with benzoyl chloride in benzene was screened utilizing 0.05 mmol of lanthanoid complex (lanthanoid (III) tris dipivaloylmethamate, Eu(dpm)_3) as a catalyst. The reaction proceeded smoothly to give *trans*-2-chlorocyclohexyl benzoate [8].



Vicinal azidoalcohols, potential precursors for β -amino alcohols and aziridines, are compounds of interest in organic synthesis. In 1999 Mizuno and Shioiri reported a novel procedure for the direct transformation of epoxide to *O*-diphenylphosphoryl vicinal azidoalcohol by the use of diphenyl phosphorazidate (DPPA, $(\text{PhO})_2\text{P(O)N}_3$) as an azidation reagent. The DPPA reacted regio- and stereoselectivity with epoxides in the presence of 4-dimethylaminopyridine (DMAP) and lithium perchlorate to give *O*-diphenylphosphoryl vicinal azidoalcohol.

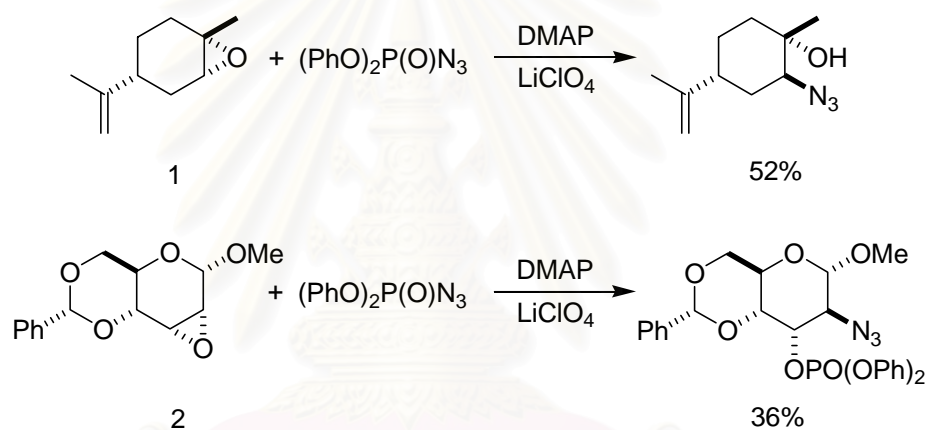


For α , β -epoxy ketones, the corresponding α -azidovinyl ketones was obtained.

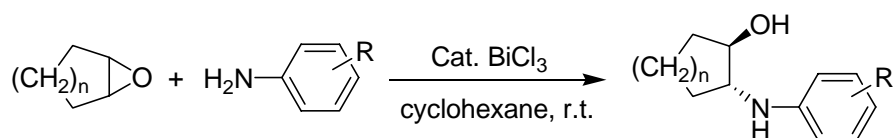


The monosubstituted and disubstituted epoxides underwent this ring opening reaction to give *O*-diphenylphosphoryl vicinal azidoalcohol in moderate to high yield. Trisubstituted epoxide (**1**) gave only the *O*-deprotected vicinal azidoalcohol. The rate of reaction depends on the structure of the employed epoxides.

2,3-Anhydro-allopyranoside (**2**) as the case of a sterically hindered epoxide, the reaction sluggishly progressed even if a stoichiometric amount of lithium perchlorate was used. The reaction carried out with new methodology was completely anti stereoselective, as shown by the presence of the anti adduct in the reaction of cyclic epoxide [9].



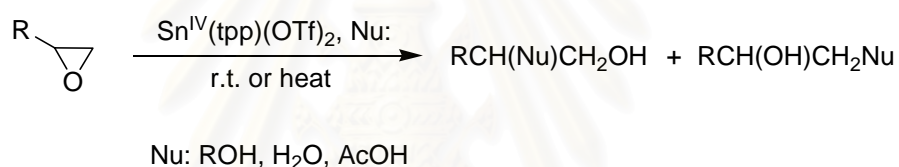
Recently, bismuth compounds have attracted the attention due to their low toxicity, low cost, and good stability. In 2002, Ollevier and Lavie-compin reported the use of bismuth trichloride as an efficient catalyst on the ring opening of epoxides. A mild and efficient procedure was performed for the ring opening of *meso*-epoxides with aromatic amines in the presence of 0.1 equivalents of bismuth trichloride as a catalyst. The corresponding *trans*- β -amino alcohols are obtained in good yields.



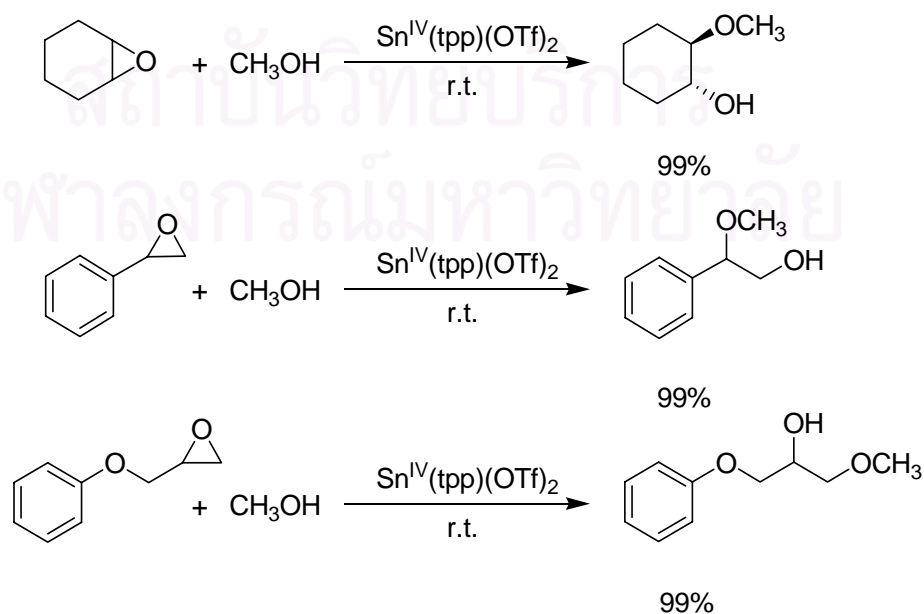
The ring opening reaction of *meso*-epoxides with more sterically hindered aromatic amine, such as *o*-methylaniline or *o*-methoxyaniline, and electron deficient amines, like *p*-trifluoromethylaniline, led also to the corresponding *trans*- β -amino alcohols in good yields [10].

The development of novel and synthetically useful chemical properties of metalloporphyrins worked as a mild and characteristic lewis acid catalyst prompted several research groups to explore the potential of electron-deficient metalloporphyrins as a catalyst for the nucleophilic ring opening of epoxides.

In 2004 Moghadom and colleagues reported that the newly synthesized tin (IV) tetraphenylporphyrinato trifluoromethanesulfonate $\text{Sn}^{\text{IV}}(\text{tpp})(\text{OTf})_2$, a stable Sn(IV) compound, could act as an efficient catalyst for the alcoholysis, hydrolysis and acetolysis.

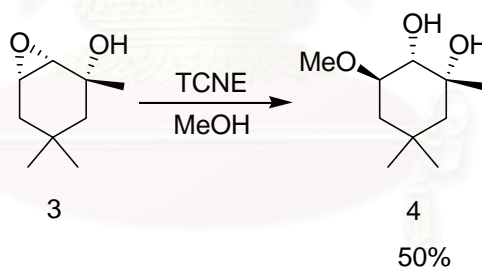


The alcoholysis of *meso* epoxides and unsymmetrical epoxides, such as cyclohexene oxide, styrene oxide and 2,3-epoxypropylphenyl ether with methanol, was catalyzed by 0.019 mol equivalent $\text{Sn}^{\text{IV}}(\text{tpp})(\text{OTf})_2$, affording the corresponding β -alkoxy alcohols in high yield.

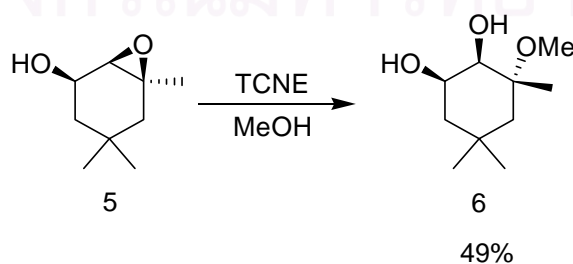


The reactions in the case of cyclohexene oxide were stereoselective and only *trans* product was obtained. In the case of unsymmetrical epoxides, 2,3-epoxy-propyl phenyl ether, the reactions were regioselective with an attack of the nucleophile (alcohol) on the less substituted oxirane carbon to yield the anti Markovnikov type products while styrene oxide, in which the reactions occurred on the more substituted carbon; Markovnikov type products were obtained. The reaction of these epoxides with acetic acid in the presence of 0.019 mol equivalent of $\text{Sn}^{\text{IV}}(\text{tpp})(\text{OTf})_2$ occurred in the same manner as alcohols with high yields of the corresponding β -acetoxy alcohols [11].

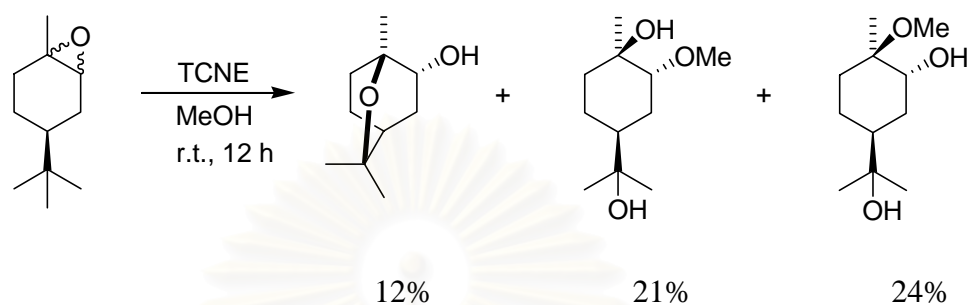
In 2005 Uyanik and colleagues reported that the regiochemistry and stereochemistry of tetracyanoethylene (TCNE) catalyzed methanolysis of some cyclohexene epoxides were directed by the presence of a hydroxyl group such as isomeric *cis*-2,3-epoxy-1,5,5-trimethylcyclohexan-1-ol (**3**) and *cis*-1,2-epoxy-1,5,5-trimethylcyclohexan-3-ol (**5**). Methanolysis of (**3**) catalyzed by TCNE gave *cis*-1,2-dihydroxy-*trans*-3-methoxy-1,5,5-trimethyl cyclohexane (**4**).



Methanolysis of (**5**) catalyzed by TCNE gave a single product, *cis*-2,3-dihydroxy-*trans*-1-methoxy-1,5,5-trimethylcyclohexane (**6**)



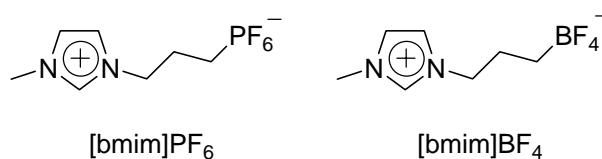
The TCNE catalyzed methanolysis of the mixed epoxides of α -terpineol gave three major products as below.

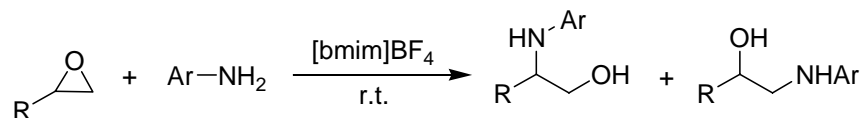


The stereochemistry of the products was established by X-ray crystallography. The structures of these products indicated that when using TCNE was used as a mild π -acid catalyst for the cleavage of hydroxyl-epoxides, the hydroxyl group could participate in the reaction [12].

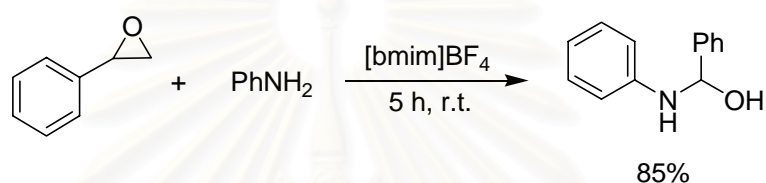
To minimize the amount of harmful organic solvents, much attention has been devoted to the use of alternative reaction media. Ionic liquids have shown great promise as attractive alternatives to conventional solvents and emerged as alternative reaction media for the immobilization of transition metal base catalysts and Lewis acids. They possess unique properties such as tunable polarity, high thermal stability, immiscibility with a number of organic solvents, negligible vapour pressure and ease of recovery and reuse of these ionic solvents. These advantages ionic liquids can make a significant contribution to green chemistry.

In 2002 Yodav and colleagues reported the use of ionic liquids 1-butyl-3-methylimidazolium tetrafluoroborate ([bmim]BF₄) or 1-butyl-3-methylimidazolium hexafluorophosphate ([bmim]PF₆) as efficient promoters for the opening of epoxides with aryl amines under mild and neutral conditions to afford the corresponding β -amino alcohols.

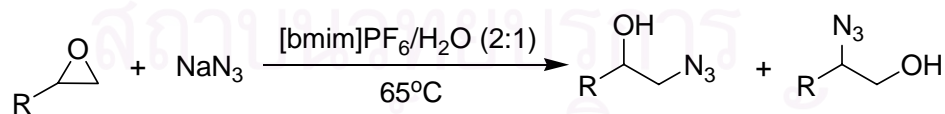




The reaction of styrene oxide with aniline in 1-butyl-3-methylimidazolium tetrafluoroborate ionic liquid at ambient temperature afforded the corresponding 2-aminophenyl-2-phenyl-1-ethanol in excellent yields with high regioselectivity [6].



2-Azidoalcohols are important precursors for the synthesis of β -amino alcohols. They have become increasingly useful and important in drugs and pharmaceuticals. The development of simple, efficient and environmentally friendly processes for their synthesis is desirable. In 2005 Yadav and colleagues reported the use of ionic liquids/H₂O ([bmim]BF₄/H₂O or [bmim]PF₆/H₂O (2:1)). Solvent system as an effective reaction medium for the synthesis of 2-azidoalcohols from ring opening of oxirane. The reaction underwent smoothly with sodium azide (NaN₃) under mild and neutral conditions in excellent yields.

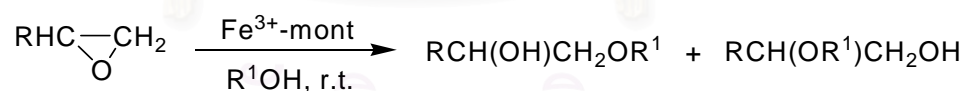


The epoxides showed a significant increase in reactivity, thereby reducing the reaction times and improving the yields substantially. Simple experimental and product isolation procedures combined with ease of recovery and reuse of this reaction media was expected to contribute to the development of green strategy for the preparation of 2-azidoalcohols [13].

1.1.2 Reactions with heterogeneous catalysts

Heterogeneous catalysts are increasingly playing an important role in organic synthesis compared to homogeneous catalysts. Nafion-H, dehydrated alumina [14] and organotin phosphate condensates [15] as heterogeneous catalysts have achieved limited success in ring opening reactions of epoxides but they suffered from serious disadvantage *i.e.*, high acidity, non catalytic nature of the reagent and inconvenient handling. The development of an efficient heterogeneous catalyst for the opening of epoxide ring has been an important goal for organic synthesis and industrial point of view.

In 1996 Choudary and Sudha reported the new methodology involving Fe^{3+} -exchanged montmorillonite catalyst for alcoholysis of epoxide ring to increase selectivity and offer many advantages over the existing methodologies. For instance, montmorillonite is cheaper, abundantly available in nature, the reaction time is very short, high yields and high selectivity, mild reaction conditions, the ease of work up and easy regeneration of the catalyst without loss of its activity. Fe^{3+} -exchanged montmorillonite has shown to be a very efficient catalyst for regio- and stereoselective alcoholysis of epoxide in primary, secondary and tertiary alcohols. The ring opening reactions are completely regioselective affording corresponding β -alkoxy alcohol as the sole regioisomer [16].



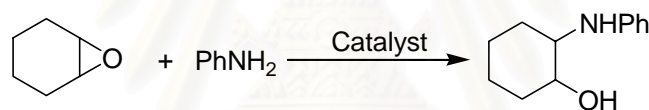
In 1994 Iranpoor and Zardaloo found that tristrinitrato [Ce(IV)paraperiodate] (TTCPP) is an efficient catalyst for the ring opening reaction of different types of epoxides with catalytic amounts of TTCPP in primary, secondary and tertiary aliphatic alcohols under neutral and mild conditions. The reaction gave the corresponding β -alkoxy alcohols in excellent yield with high stereo-regioselectivity [17].

Iranpoor and colleagues reported that iron (III) chloride adsorbed on chromatographic silica gel ($\text{FeCl}_3 \cdot 6\text{H}_2\text{O}/\text{SiO}_2$) could act as an efficient catalyst for alcoholysis, acetolysis and hydrolysis of epoxides under mild conditions. This catalyst

can convert epoxides to their corresponding β -alkoxy alcohols, acetoxy alcohols and diols. The reaction of epoxides with chloride, bromide and nitrate ions furnished the corresponding β -halohydrins and β -nitrate alcohols in excellent yield with high regio- and stereoselectivity [18].

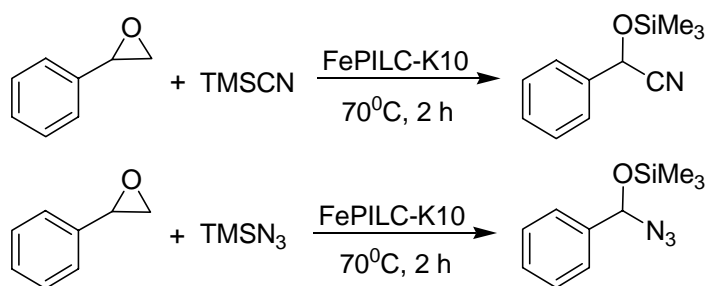


In 2000 Kantam and colleagues tested the catalytic nucleophilic ring opening of cyclohexene oxide with aniline catalyzed by different K-10 montmorillonite catalysts such as K-10 montmorillonite, FeCl₃-exchanged K-10 montmorillonite and Fe-pillared K-10 (FePILC-K10). It was found that FePILC-K10 showed higher isolated yield and shorter reaction time than FeCl₃-exchanged K-10 and montmorillonite K-10, respectively [19].

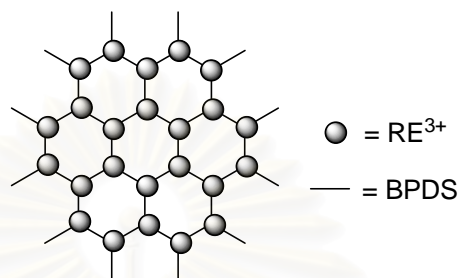


Catalyst	Reaction time (h)	Isolated yield (%)
1) K-10 montmorillonite	36	50
2) Fe-exchanged K-10	4	79
3) FePILC-K10	1.5	95

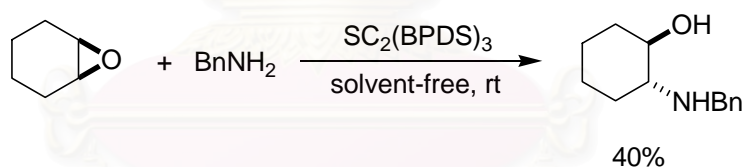
The efficiency of FePILC-K10 was evident from the high yields obtained for the ring opening reaction of oxirane with TMSCN and TMSN₃ as a nucleophile.



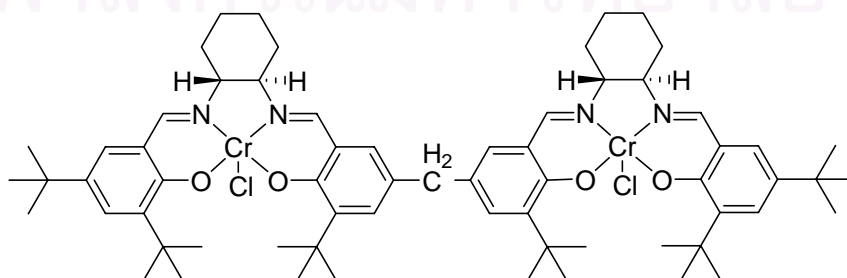
In 2005 Ishida and colleagues reported the use of novel polymeric rare earth complexes (scandium (III) biphenyl-4,4'-disulfonate, $SC_2(BPDS)_3$) for the ring opening reaction of epoxides with amines.



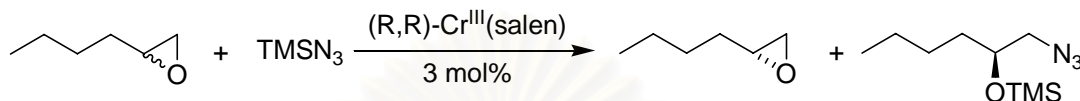
The scandium (III) biphenyl-4,4'-disulfonate was successfully used as a reusable Lewis acid catalyst for ring opening of cyclohexene oxide with benzylamine ($BnNH_2$) under solvent-free heterogeneous conditions to give *trans*-2-benzylamino-1-cyclohexanol in excellent yields. The catalyst can be quantitatively recovered after the reaction and reused more than five times without decreasing their catalytic activities [20].



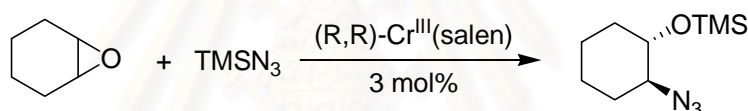
In 2005 Dioso and Jacobs reported the attempt to synthesize a dimeric $Cr^{III}(salen)$ complex and immobilize it on silica by impregnation as a catalyst for the asymmetric ring opening reaction of epoxides.



The reaction of the terminal epoxide such as 1,2-epoxyhexane with trimethylsilylazide (TMSN_3) as a nucleophile was screened utilizing 3 mol% of dimeric $\text{Cr}^{\text{III}}(\text{salen})$ on silica as a catalyst. The kinetic resolution of 1,2-epoxyhexane resulted in excellent reactivity and very high levels of enantioselectivity.



For other *meso* epoxides, such as cyclohexene oxide and cyclopentene oxide with TMSN_3 , epoxide fused to six-membered ring underwent ring opening with high 100% conversion, while epoxide fused to five membered ring revealed lower conversion but higher enantioselectivity [21].

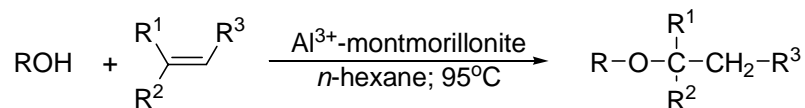


1.2 Literature review on clay catalysts

Clay catalysis may function as Bronsted or Lewis acids. Organic reactions that take place under acid catalysis can be very efficiently carried out using clay catalysts. These reactions are more efficiently, under milder conditions, with greater selectivity, better yields and shorter reaction times. Moreover, the work up and purification procedures are simple as the catalyst can be filtered or centrifuged out from the reaction mixture. The range of reactions successfully performed on clay catalysts include addition, elimination, substitution, rearrangement, Diels-Alder reaction, oxidation-reduction, ring opening reaction [22], oligomerization, dehydration and Friedal-Crafts reaction [23].

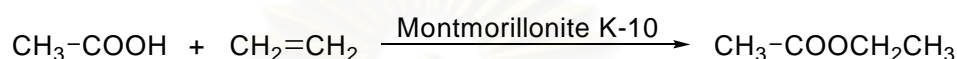
Ether formation

Unsymmetrical ethers were efficiently prepared by refluxing a solution of alcohol and olefin in *n*-hexane using Al^{3+} -exchanged montmorillonite. The yields were good in the case of primary alcohols. Secondary alcohols gave low yields, while tertiary alcohols did not yield to ethers, because dehydration occurs more easily [23].

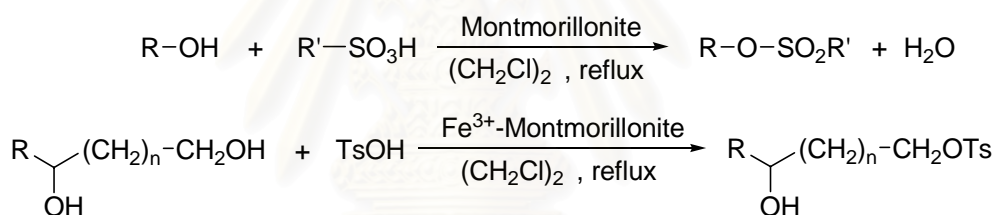


Esterification

Addition of carboxylic acid to an olefinic compound leading to ester was brought about in acid-activated montmorillonite clay as indicated below.

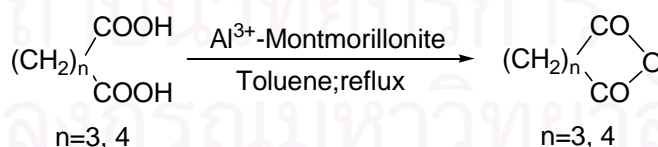


In an analogous manner, tosyl or sulphonyl esters were prepared in good yields by refluxing alcohols with sulphonic acids using Fe^{3+} -montmorillonite in ethylene dichloride solvent. Diols can be selectively monotosylated [22].



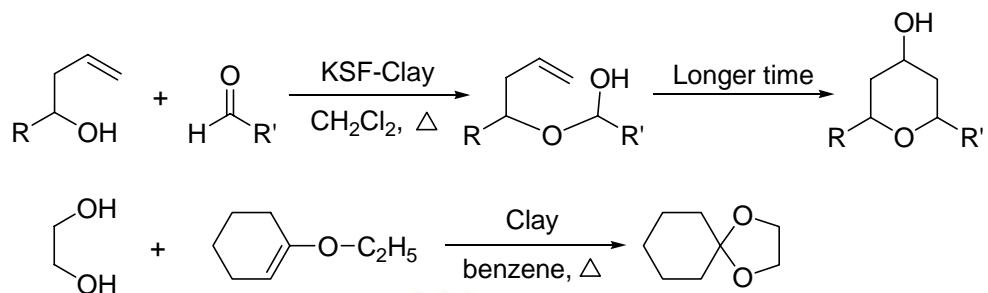
Anhydride formation

The facile dehydration reaction in acid clay medium led to the formation of cyclic anhydrides from 5- and 6-carbon dicarboxylic acids [22].



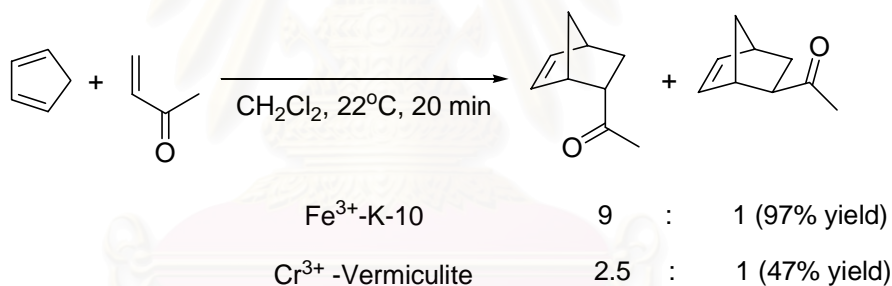
Reactions of alcohols with ketones and aldehydes

Addition of alcohols to carbonyl compounds occurred easily in the presence of montmorillonite clays. Acetals were prepared by taking advantage of this fact. Recently, homoallyl alcohols have been observed to add to aldehydes leading to hemiacetal intermediates, which further undergo intramolecular transformation to give Prins-type cyclization products [22].



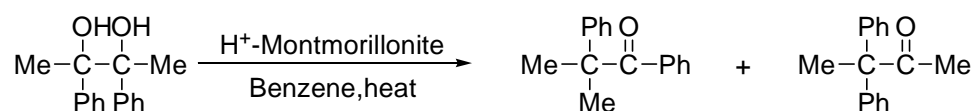
Diels-Alder reaction

Although the Diels-Alder reaction is a thermally allowed [4+2] cycloaddition process, it does not occur spontaneously with all dienes and dienophiles. The rates of these slow reactions can be greatly accelerated when they are carried out using clay catalysts even under very mild conditions. The catalytic character of clays in these reactions is due to their acidic property [22].

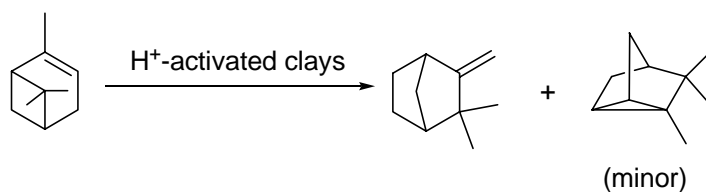


Rearrangement reaction

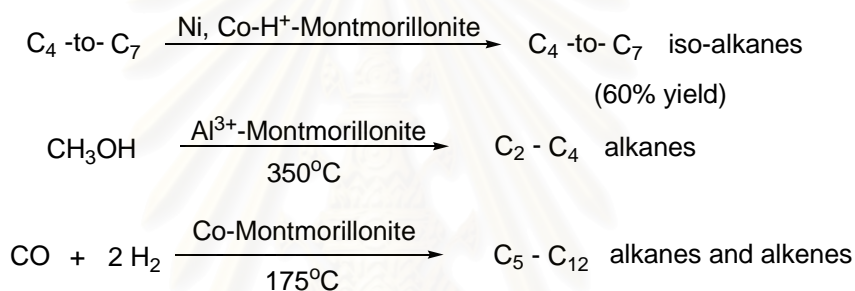
A good number of rearrangement/isomerization reactions have been carried out using clay catalysts. For example, pinacol-pinacolone reaction is a common reaction of tertiary 1,2-glycols catalyzed by acids, in which an alkyl or an aryl group migrates to an adjacent position [22].



For example, the isomerizations of α -pinene to camphene and lonifolene to isolongifolene have been carried out in good yields on acid-treated montmorillonite.

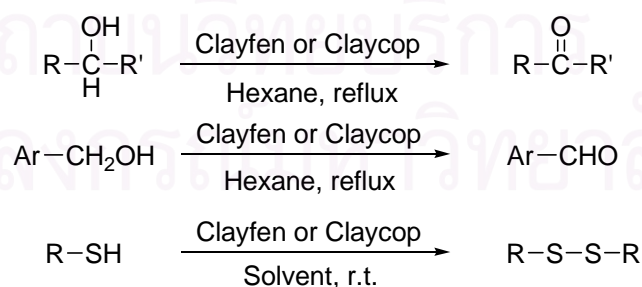


Petroleum cracking is an important industrial application in petrochemical processing. Pillared clays could be used in this process since they are more stable at high temperature. Catalytic reforming and isomerization of *n*-alkanes to branched chain alkanes increases the octane number. Conversion of methanol to alkanes and of synthesis-gas to hydrocarbons has also been achieved.



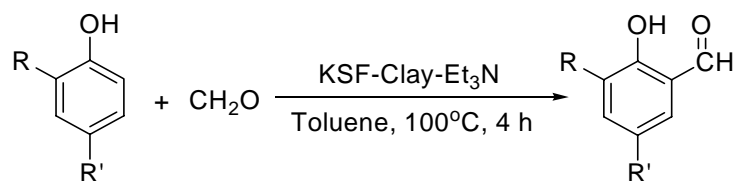
Oxidation-reduction reaction

Clayfen and claycop are K-10 clay supported iron(III) nitrate and copper(II) nitrate reagents, respectively. Both are excellent oxidizing reagents for alcohols, thio-compounds and many others [22].



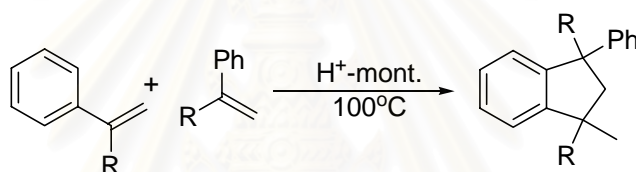
Formylation of phenols

Phenols could be formylated by reaction with formaldehyde using clay catalyst and R_3N [22].



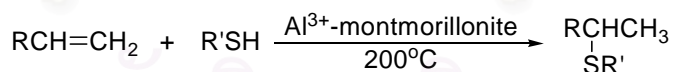
Oligomerization reaction

Alkenes underwent oligomerization in the presence of acid-treated or ion-exchanged montmorillonites. The reaction involved protonation to generate a stabilized carbocation that reacted with other alkene molecules to give dimers as well as oligomers after deprotonation. The polymerization of styrene has been catalyzed by acid-treated montmorillonites [23].



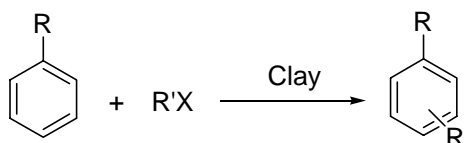
Addition reaction

Thiol and hydrogen sulfide can add to alkenes in the presence of montmorillonite to afford dialkyl sulfides in good yields [23].



Aromatic electrophilic substitution (Friedel-Crafts reaction)

Montmorillonite supported transition metal salts (zinc and nickel chlorides) are highly active and selective reagents for the catalysis of Friedel-Crafts alkylation [23].



From these literature reviews, epoxides are one of the most important intermediates in organic synthesis. The importance in the reaction of epoxides ring opening involved the use of lewis acid and lewis base. The development of a more efficient heterogeneous catalyst for the opening of epoxide ring has been an important goal for organic synthesis and industrial point of view. Clay catalysts have been reported as an efficient catalyst in the epoxide ring opening. Although there have been some investigations on the use of Fe^{3+} -exchange clay for catalytic ring opening of epoxide, there is no report on the utilization of Fe-pillared clay as a catalyst. This research concerned with the selectively catalytic ring opening by Fe-pillared bentonite and Fe-pillared hectorite under mild conditions.

1.3 The goal of this research

1. To synthesize the efficient iron oxide-pillared clay catalyst for ring opening of styrene oxide.
2. To study the optimum conditions for epoxide ring opening, using styrene oxide as a model substrate and the selected iron oxide-pillared clay as a catalyst.
3. To apply the optimum conditions for the ring opening of some selected epoxides.

CHAPTER II

THEORY

2.1 Clay

Clay minerals are crystalline hydrous aluminosilicates, classified as phyllosilicates, or layered silicate structures. They occur abundantly in nature. The unique properties of clays contain high surface area, high sorption, reversible ion-exchange and high acidity. Their acidity as both brønsted and lewis types has been exploited for catalytic applications. Many organic reactions use clays as an efficient heterogeneous catalyst. For example, modified smectite clays could be used as highly selective catalysts in organic transformations and green chemistry with excellent yield, high regio- and stereoselectivity. The advantage of clay catalysts over homogeneous catalyst shows at the work up of the reaction mixture which are very simple by filtration [24].

2.2 The structure of clay minerals

Clay minerals possess a layered structure, and their suspension in aqueous solution contains particles with the average diameter of about 2 μm [25]. The layered units are constructed from the combination of two basic types of layers: a sheet of corner linked tetrahedra and a sheet of edge-linked octahedra. Phyllosilicate minerals have layered structures composed of aluminum octahedral and silica tetrahedral sheets. The tetrahedral and octahedral sheets are held together by sharing apical oxygen atoms [26].

2.2.1 Basic units

2.2.1.1 Tetrahedral sheets

In tetrahedral sheet, the dominant cation is Si^{4+} (SiO_2), but frequently substituted by Al^{3+} and occasionally by Fe^{3+} . This sheet extends infinitely in two dimensions by each tetrahedron sharing three oxygens with three other tetrahedra to form hexagonal network (Figure 2.1). They are arranged in a hexagonal pattern with the basal oxygens linking and the apical oxygens pointing up/down.

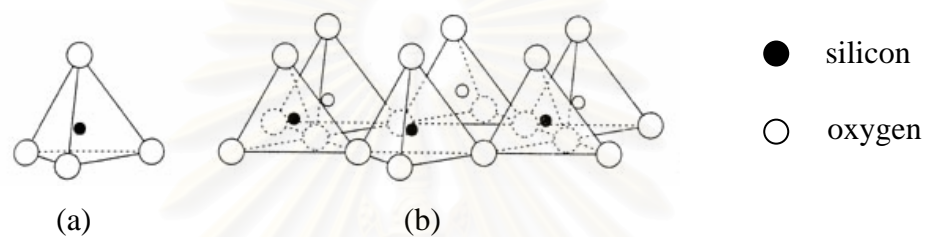


Figure 2.1 A single tetrahedral silica (a), and a sheet structure of silica tetrahedra arranged in a hexagonal network (b).

2.2.1.2 Octahedral sheets

The octahedral sheet is composed of as two planes of closest-packed oxygen ions with cation occupying the resulting octahedral sites between two planes (a). The dominant cation is Al^{3+} , but substituted frequently by Mg^{2+} and occasionally by Fe^{2+} and Fe^{3+} . Connection of the neighboring oxygen ions forms a sheet of edge-linked octahedra as hexagonal network, extending infinitely in two dimensions (b).

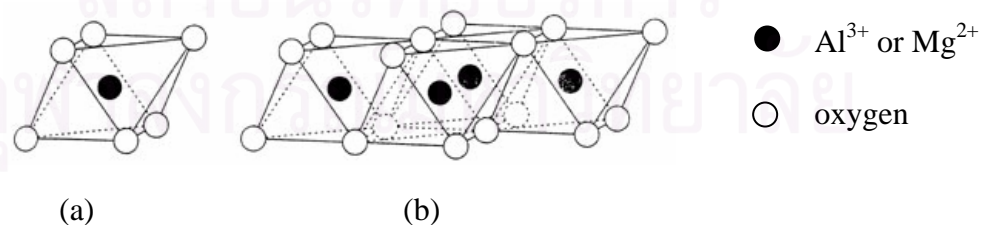


Figure 2.2 A single octahedral unit (a), and a sheet structure of octahedral unit arranged in hexagonal network (b).

2.2.2 The combinations of basic sheets

The combinations of basic sheets of clays could be divided into 2 categories:

2.2.2.1 The 1:1 layered type (T:O)

This combination of one tetrahedral sheet (T) and one octahedral sheet (O) is one unit of clay layer. The oxygen atoms at the edge of tetrahedral sheet are pointed to the octahedral sheet and held together with sharing those atoms.



Figure 2.3 Structure of 1:1 layered type (T = tetrahedral sheet, O = octahedral sheet).

Kaolinite is the most common in this type of clay and has the chemical formula $\text{Al}_2\text{Si}_2\text{O}_5(\text{OH})_4$. It consists of an octahedrally coordinated layer of aluminum ions and a layer of tetrahedrally coordinated silicon atoms in 1:1 structure. Kaolinite layers are held together by Van der Waals forces. The thickness of each clay layer is about 7 \AA , which gives rise to a corresponding characteristic X-ray diffraction peak of about 7 \AA .

2.2.2.2 The 2:1 layered type (T:O:T)

A 2:1 layer of clay minerals is composed of two silica tetrahedral layers with one alumina octahedral layer in between. This combination makes a tetrahedral-octahedral-tetrahedral (T:O:T) sandwich. Pyrophyllite $[\text{Al}_2\text{Si}_4\text{O}_{10}(\text{OH})_2]$ and talc $[\text{Mg}_3\text{Si}_4\text{O}_{10}(\text{OH})_2]$ are the simplest members of this group.

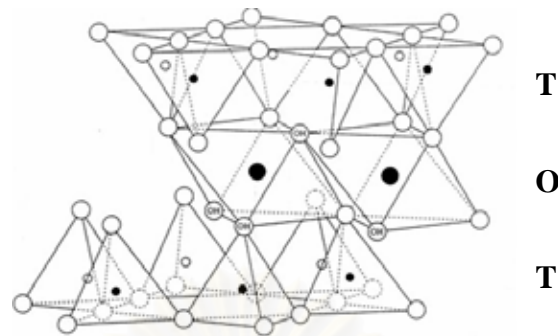


Figure 2.4 Structure of 2:1 layered type (T = Tetrahedral sheet, O = Octahedral sheet).

2.3 Smectite clay minerals [27]

Smectite clays are a family of expandable 2:1 phyllosilicate clay minerals, and are derived from the mineral talc and pyrophyrite which consist of a stacking of charged-neutral layers of the composition $\text{Mg}_6\text{Si}_8\text{O}_{20}(\text{OH})_4$ and $\text{Al}_4\text{Si}_8\text{O}_{20}(\text{OH})_4$, respectively. Cation substitution in either the octahedral sheet (typically from the substitution of low charge species such as Mg^{2+} , Fe^{2+} or Mn^{2+} for Al^{3+}) or tetrahedral sheet (Al^{3+} or occasionally Fe^{3+} substitutes for Si^{4+}) results in negative layered charge, which is balanced by additional cations locating between the interlayer of clay. The interlayer is hydrated, which cations to move freely in and out of the structure.

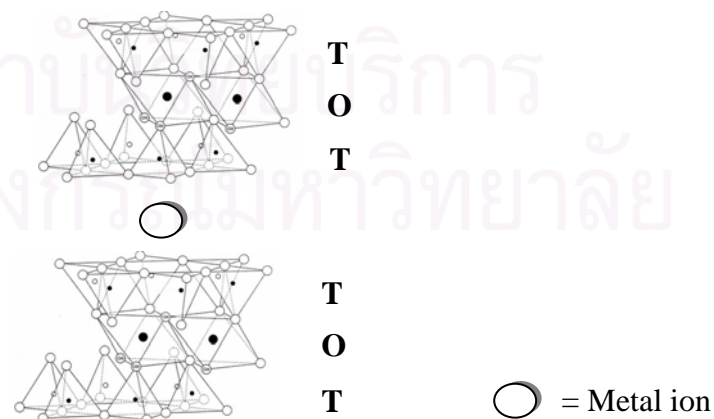


Figure 2.5 Structure of smectite clay.

The most important ability of the smectite group is the adsorption of a large amount of water molecules between the layers, causing the volume of the minerals increase. Thus, the smectites are expanding clays with the basal spacing of 10 to 20 Å.

The most common smectite is montmorillonite with a general chemical formula of $(\frac{1}{2}\text{Ca,Na})(\text{Al,Mg,Fe})_4(\text{Si,Al})_8\text{O}_{20}(\text{OH})_4 \cdot n\text{H}_2\text{O}$.

Smectite clays normally occur as extremely small crystals (less than 1 µm), so the identification is usually based on X-ray diffraction technique.

2.3.1 Bentonite clay [28]

Montmorillonite, $(\text{Si}_8)(\text{Al}_{4-x}\text{Mg}_x)\text{O}_{20}(\text{OH})_4\text{A}_x \cdot n\text{H}_2\text{O}$, is the main constituent of bentonite, derived by weathering of volcanic ash Mg/Al substitution in the octahedral sheet gives the clay layer negative charged. Montmorillonite can expand by several times of its original volume when it adsorbs water.

2.3.2 Hectorite clay [28]

The octahedral sheet of hectorite is contained of Mg^{2+} , which is different from bentonite. Hectorite has Li/Mg substitution in the octahedral sheet, resulting to negatively charged layers. The general formula of hectorite is $(\text{Si}_8)(\text{Mg}_{6-x}\text{Li}_x)\text{O}_{20}(\text{OH})_4\text{A}_x \cdot n\text{H}_2\text{O}$ (where A is a monovalent or divalent cation).

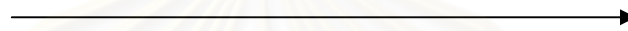
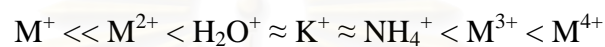
2.4 Properties of clay

2.4.1 Ion exchange [24]

Clays have the ability to adsorb and exchange cations from solution. In most clays, the ideal neutral structure is disrupted by introduction of charged imbalance into the clay sheets. Two main causes of these charged imbalance are (1) isomorphous substitution of cations in the lattice by lower valent ions, such as the substitution of aluminum cation for silicon in the tetrahedral layer, magnesium for aluminum or sometimes lithium for magnesium cations in the octahedral layer and (2) crystal defects. The layers have an overall negative charge which is balanced by adsorption of metal cations into the interlayer of the clay minerals. These balance cations can be readily replaced by other cations in aqueous solution. The property of ion exchange is great fundamental and practical importance in the investigation of clay minerals. In

the application of clay mineralogy, it is important because the nature of the exchangeable ion may influence substantially the physical properties of the material.

When a solution of a metal cation is used to exchange the interlayer cations of clay, it has been observed that the smaller the size and the higher the charge of the exchange cation, the more powerful that cation at replacing the interlayer exchangeable cations. Similarly the ease of replacement of interlayer cations follows the reverse trend. The following series can be constructed:



increasing exchange power
(decreasing ease of exchange)

Figure 2.6 The exchange properties of cations with clays.

For the swelling clay minerals, such as smectites, the interlayer cations can be exchanged with cations from external solutions.

The concentration of exchangeable cations (CEC) is measured in milliequivalents per 100 g of dried clay. CEC is often measured by uptake and release of ammonium ions from 1 M ammonium acetate solution, although other cations are sometimes used in place of NH_4^+ . Since smectites have the highest concentration of interlayer cations, they have the highest cation exchange capacities (typically 70-120 mequiv/100 g). Structural defects at layer edges give rise to additional CEC and a small amount of anion exchange capacity [23].

2.4.2 Swelling [23]

Many clay minerals adsorb water between their layers, which move apart and the clay swells. The energy is released by the attractive forces, such as hydrogen bonding, between the adjacent layers from cations and/or layer solvation. Thus water forms strong hydrogen bonds with hydroxyl groups on hydrophilic octahedral layers in 1:1 clay minerals (kaolinite), allowing swelling to occur.

With 2:1 clay minerals, the ability to swell depends on the solvation of interlayer cation and layer charge. Clays with 2:1 structures and low layer charge have very low concentration of interlayer cations and therefore do not swell readily. At the other extreme, those with very high layer charges have strong electrostatic forces holding alternate anionic layers and the interlayer cations together, thus preventing swelling. Those with univalent interlayer cations swell most readily. For those with divalent, trivalent and polyvalent cations, swelling decrease accordingly. The extent of swelling can be observed by measuring interlayer separations using power X-ray diffraction.

2.4.3 Acidity of clays [24]

Clay minerals show both Brønsted and Lewis acidity. The interlayer cations contribute to the acidity of clay minerals. Some of these cations may be protons or polarizing cations (*e.g.* Al^{3+}) which give rise to strong Brønsted acidity. The higher electronegativity of M^+ , the stronger acidic sites generated. Brønsted acidity also stems from the terminal hydroxyl groups and from the bridging oxygen atoms. In addition, clay minerals have layer surface and edge defects, which would result in weaker Brønsted and/or Lewis acidity, generally at low concentrations.

A further source of acidity is associated with the $-\text{OH}$ groups of the octahedral layer which protrude into the interlayer region *via* the holes of the ring. The incidence of these protons may be increased by preparing a 'proton-exchanged' clay. This is achieved either a simply exchanging the clay with dilute acid, or less destructively to exchanging the clay with ammonium ions and calcining at 200-300°C to expel ammonia. The exchanged proton can migrate into vacancies on the octahedral layer where they protonate bridging oxygen.

2.5 Intercalation [29]

Intercalation is the insertion of a guest species into the interlayer region of a layered solid, and consequently the layered structure still remains. Intercalation compound is proven by the XRD pattern, which must unambiguously show an increase in the spacing between adjacent layers, *i.e.* an increase in the basal spacing.

2.6 Pillaring [29]

Pillaring is the process by which a layered compound is transformed into a pillared compound or a pillared layered solid which is thermally stable micro- and/or mesoporous material with retention of the layer structure. A pillared derivative is distinguished from an ordinary intercalate by virtue of intracrystalline porosity made possible by the lateral separation of the intercalated guest.

2.7 Pillared clay (PILCs)

Pillared interlayer clays, a family of microporous materials, was prepared by exchanged cations and polyoxocations bulk in organic into the interlayer of swellable clay, leading to the intercalated clays. The intercalated clays are calcined, the polyoxocations are transformed into pillars, thus leading to the pillared solids. The possibility of controlling the properties of the pillared solids are performed by changing the clay nature (montmorillonite, bentonite, hectorite, *etc*) and the intercalating species nature (polycations based on Al^{3+} , Si^{4+} , Ti^{4+} , Zr^{4+} , Cr^{3+} , Fe^{3+} or Ca^{2+} , *etc*) [30]. The resulting material has a high specific surface area and a characteristic porous structure which is of great interest because of its potential application in various fields [31].

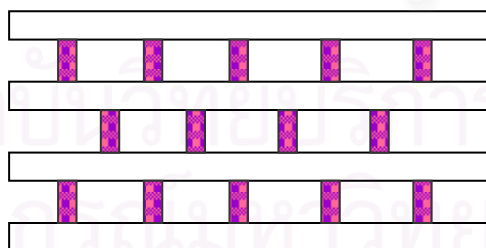


Figure 2.7 The model of pillared clay structure (cross section).

2.7.1 Pillaring agent [29]

A pillaring agent is any compound, which can be intercalated between adjacent layers of a layered compound. It maintains the spacing between adjacent

layers upon removal of the solvent and induces an experimentally observable pore structure between the layers.

2.8 Characterization of clays and clay catalysts

2.8.1 Powder X-ray diffraction (XRD) [26]

X-ray powder diffraction (XRD) is an instrumental technique that is used to identify minerals, as well as other crystalline materials. XRD is a technique in which a collimated beam of nearly monochromatic X-rays is directed onto the flat surface of a relatively thin layer of finely ground material. XRD can provide additional information beyond basic identification. If the sample is a mixture, XRD data can be analyzed to determine the proportion of the different minerals present. Other information obtained can include the degree of crystallinity of the minerals present, possible deviations of the minerals from their ideal compositions, the structural state of the minerals and the degree of hydration for minerals that contain water in their structure. Figure 2.8 shows a monochromatic beam of X-ray incident on the surface of crystal at an angle θ . The scattered intensity can be measured as a function of scattering angle 2θ . The resulting XRD pattern efficiently determines the different phases present in the sample.

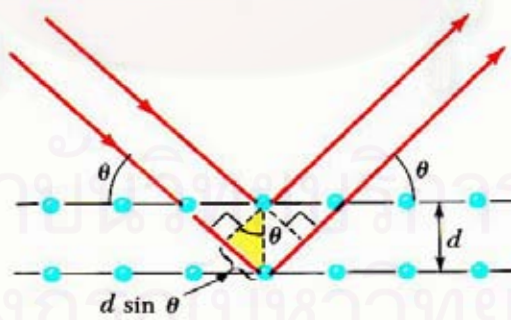


Figure 2.8 Diffraction of X-ray by regular planes of atoms.

Using this method, Bragg's law is able to determine the interplanar spacing of the samples, from diffraction peak according to Bragg angle.

$$n\lambda = 2d \sin\theta$$

Where the integer n is the order of the diffracted beam, λ is the wavelength, d is the distance between adjacent planes of atoms (the d -spacings) and θ is the angle of between the incident beam and these planes.

2.8.2 Nitrogen adsorption-desorption isotherm

The N_2 adsorption technique is used to determine the physical properties of mesoporous molecular sieves, such as the surface area, pore volume, pore diameter and pore-size distribution of solid catalysts.

Adsorption of gas by a porous material is described by an adsorption isotherm, the amount of adsorbed gas by the material at a fixed temperature as a function of pressure. Porous materials are frequently characterized in terms of pore sizes derived from gas sorption data. IUPAC conventions have been proposed for classifying pore sizes and gas sorption isotherms that reflect the relationship between porosity and sorption. The IUPAC classification of adsorption isotherms is illustrated in Figure 2.9. Six types of isotherms are characteristic of adsorbents that are microporous (type I), nonporous or macroporous (types II, III, and VI) or mesoporous (types IV and V) [32].

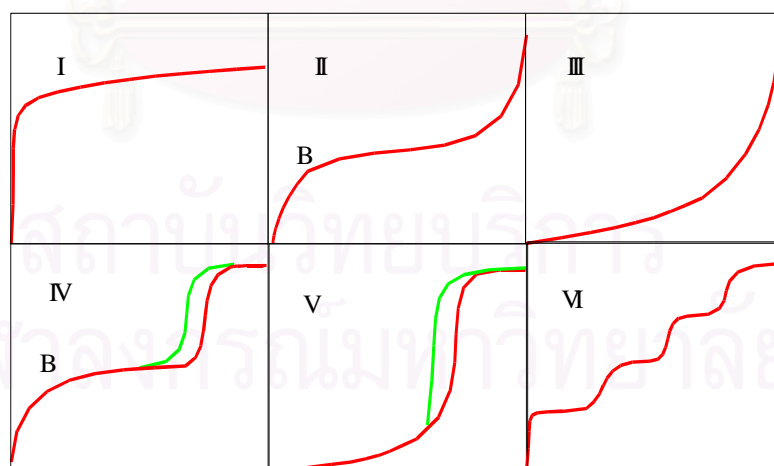


Figure 2.9 The IUPAC classification of adsorption isotherm.

Adsorption isotherms are described as shown in Table 2.1 based on the strength of the interaction between the sample surface and gas adsorbate, and the existence or absence of pores. Pore types are classified as shown in Table 2.2 [33].

Table 2.1 Features of adsorption isotherms

Type	Features	
	Interaction between sample surface and gas adsorbate	Porosity
I	Relatively strong	Micropores
II	Relatively strong	Nonporous
III	Weak	Nonporous
IV	Relatively strong	Mesopore
V	Weak	Micropores or Mesopore
VI	Relatively strong Sample surface has an even distribution of energy	Nonporous

Table 2.2 IUPAC classification of pores

Pore Type	Pore diameter / nm
Micropore	Up to 2
Mesopore	2 to 50
Macropore	50 to up

Pore size distribution is measured by the use of nitrogen adsorption/desorption isotherm at liquid nitrogen temperature and relative pressures (P/P_0) ranging from 0.05-0.1. The large uptake of nitrogen at low P/P_0 indicates filling of the micropores ($<20 \text{ \AA}$) in the adsorbent. The linear portion of the curve represents multilayer adsorption of nitrogen on the surface of the sample, and the concave upward portion of the curve represents filling of mesopores and macropores.

The multipoint Brunauer, Emmett and Teller (BET) method is commonly used to measure total surface area.

$$\frac{1}{W[(P_o/P)-1]} = \frac{1}{W_m C} + \frac{C-1}{W_m C} (P/P_o)$$

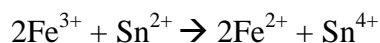
Where W is the weight of nitrogen adsorbed at a given P/P_o , and W_m is the weight of gas to give monolayer coverage, and C is a constant that is related to the heat of adsorption. A linear relationship between $1/W[(P_o/P)-1]$ and P/P_o is required to obtain the quantity of nitrogen adsorbed. This linear portion of the curve is restricted to a limited portion of the isotherm, generally between 0.05-0.30. The slope and intercept are used to determine the quantity of nitrogen adsorbed in the monolayer and calculate the surface area. For a single point method, the intercept is taken as zero or a small positive value, and the slope from the BET plot is used to calculate the surface area. The surface area reported depend upon the method used, as well as the partial pressures at which the data are collected.

2.8.3 Determination of iron content in sample [34]

Analysis of iron compound was performed by Zimmermann-Reinhardt method. Steps in the analysis of sample are (1) decomposition of the sample, (2) reduction of iron to the divalent state, (3) removal of excess reductant, and (4) titration of iron(II) with a standard oxidant.

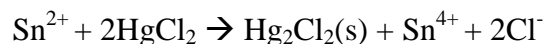
The decomposition of the sample: iron oxides are often decomposed completely in hot concentrated HCl. The rate of attack by this reagent is increased by the presence of a small amount of tin(II) chloride which probably acts by reducing solution iron(III) oxides of the sample to more soluble iron(II) species.

The reduction of iron: because part of the iron is in the trivalent state after decomposition of the sample, reduction to iron(II) must precede titration with the oxidant. The Zimmermann-Reinhardt method uses tin(II) chloride as a pre-reductant for iron. Tin(II) chloride is added dropwise to the disappearance of the yellow color of Fe(III).



The other common species reduced by this reagent are the high oxidation states of arsenic, copper, mercury, molybdenum, tungsten, and vanadium.

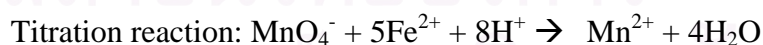
The removal of excess reductant: the slight excess of tin(II) chloride is eliminated by the addition of mercury(II) chloride:



Element mercury reacts with permanganate and causes the results of analysis to be high. The formation of mercury, which is favored by an appreciable excess of tin(II), is prevented by careful control of this excess and by the rapid addition of excess mercury(II) chloride. A proper reduction is indicated by the appearance of a small amount of a silky white precipitate after the addition of mercury(II). Formation of a gray precipitate at this juncture indicates the presence of metallic mercury or the total absence of a precipitate indicates that an insufficient amount of tin(II) chloride was used. In either event, the sample must be discarded.

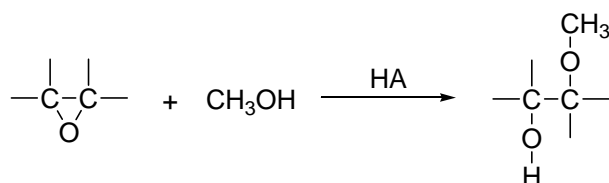
The titration of iron(II): the iron(II) solution from above is added with the Zimmermann-Reinhardt reagent, which contains manganese(II) in a fairly concentrated mixture of sulfuric and phosphoric acids.

The oxidation of chloride ion during a titration is believed to involve a direct reaction between this species and the manganese(III) ions that form as an intermediate in the reduction of permanganate ion by iron(II). The presence of manganese(II) in the Zimmermann-Reinhardt reagent is believed to inhibit the formation of chlorine by decreasing the potential of the manganese(III)/manganese(II) couple. Phosphate ion is believed to give a similar effect by forming stable manganese(III) complexes. Moreover, phosphate ions react with iron(III) to form nearly colorless complexes of $\text{Fe}(\text{PO}_4)_2^{3-}$ so that the yellow color of the iron(II)/chloro complexes does not interfere with the end point.



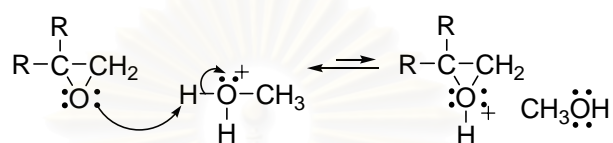
2.9 Ring-opening of epoxide under acidic conditions

Epoxides are much more reactive than ethers under acidic conditions because of their ring strain [35].

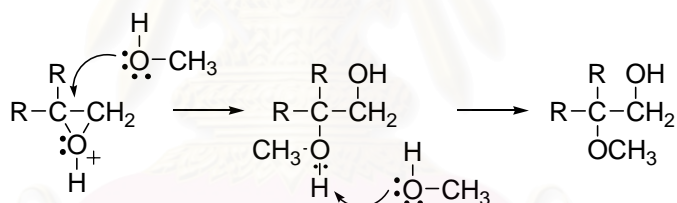


The regioselectivity of the ring-opening reaction is different under acidic and basic conditions. The structure of the product shows nucleophile methanol reacts at the more branched carbon of the epoxide. Contrast this with the reaction under basic conditions, in which the nucleophile reacts at the less branched carbon.

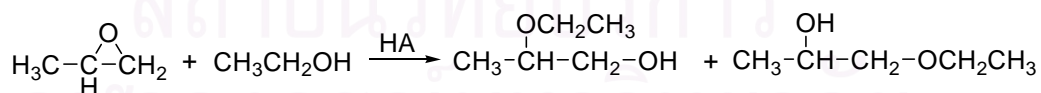
The first step in the mechanism of this reaction is protonation of the oxygen.



Consequently, the bond to the more substituted carbon is weaker than another bond to the less one. In the other word, the more substituted carbon in the protonated epoxide has a great deal of carbocation character. Then a solvent molecule attacks this carbon as it would be a carbocation to give the product after loss of a proton.



When the carbons of an unsymmetrical epoxide are secondary or primary, there is much less carbocation character at either carbon in the protonated epoxide. The reactions tend to give mixtures of product.



The mixture reflects the balance between opening of the weaker bond, which favors the attack at the more branched carbon, and steric hindrance to nucleophilic attack, which favors the attack at the less branched carbon [36].

CHAPTER III

EXPERIMENTAL

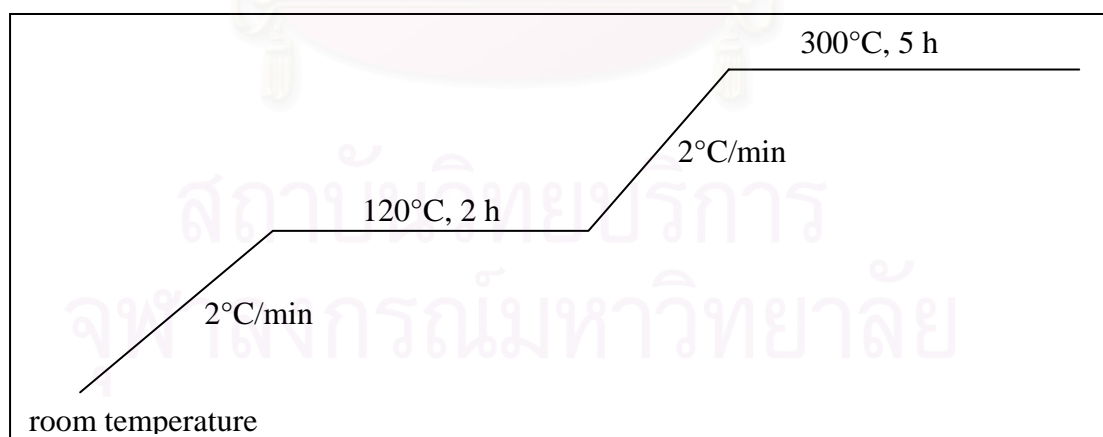
3.1 Instrument, apparatus and analytical measurements

3.1.1 Centrifuge

The purification of clays and the collection of the synthesized catalysts were processed by centaur 2, Sanyo centrifuge. The purification of clays is aimed for removing quartz and other impurities.

3.1.2 Oven and furnace

Raw clays and all synthesized catalysts were dried in a Memmert UM-500 oven at 100°C. The calcination was performed on a carbolite RHF 1600 muffle furnace in air. Calcination of assynthetic clays catalysts was conducted in order to convert metal precursors in the interlayer of clays into metal oxide. The heating program used for the calcination of Fe-pillared clays is shown in Scheme 3.1.



Scheme 3.1 The heating program used for the calcination of Fe-pillared clays.

3.1.3 X-ray diffractometer (XRD)

The XRD patterns, and consequence the basal spacings, of catalysts (raw clays, synthetic clays catalysts) were determined using a Rigaku, Dmax 2200/ultima + X-ray powder diffractometer (XRD) with a monochromater and Cu K_{α} radiation (40 Kv, 30 mA). The 2-theta angle was ranged from 2 to 30 degree with scan speed of 3 degree/min and scan step of 0.02 degree. The scattering slit, divergent slit and receiving slit were fixed at 0.5 degree, 0.5 degree and 0.15 mm, respectively.

3.1.4 Nitrogen adsorption/desorption (Brunauer-Emmett-Teller Method, BET)

The BET specific surface area of raw clays and synthesized Fe-pillared clays were measured by the Quantachrome Autosorb-1 nitrogen adsorptometer.

3.1.5 Gas chromatography (GC)

Gas chromatography analysis was carried out on a Shimadzu GC-gas chromatography equipped with a flame ionization detector (FID) with N_2 as a carrier gas and a 30-m long HP-5 column (0.25-mm outer diameter, 0.25 μ m film thickness).

3.1.6 Nuclear magnetic resonance spectroscopy (NMR)

The 1H NMR spectra were obtained in deuterated chloroform ($CDCl_3$) and determined by model Mercury plus 400 NMR spectrometer which operated at 399.84 MHz.

3.1.7 Chromatography

- Thin layer chromatography (TLC) was carried on aluminium sheets precoated with silica gel (Merck's, kieselgel 60 PF₂₅₄).
- Column chromatography was performed on silica gel (Merck's, Kieselgel 60 G).

3.2 Starting materials

3.2.1 Clays

Clays (bentonite and hectorite) were used as a raw material. Bentonite was kindly supported by Cernic International Co., Ltd. Hectorite was kindly supported by Volclay Siam Limited. The compositions of bentonite and hectorite are summarized in Table 3.1.

Table 3.1 Bentonite and hectorite compositions

	Bentonite ^a	Hectorite ^b
SiO ₂	63.60	61.78
Al ₂ O ₃	17.60	1.58
MgO	-	20.32
Fe ₂ O ₃	3.10	1.23
CaO	3.00	10.07
Na ₂ O	3.40	2.80
K ₂ O	0.50	0.33

^a information from Cernic International Co., Ltd.

^b information from Volclay Siam Limited.

3.2.2 Chemicals

1. Sodium hydroxide, NaOH (Merck, reagent grade)
2. Iron(III) chloride anhydrous, FeCl₃ (Riedel-de Haën)
3. Styrene oxide, C₈H₈O (Fluka, 97%)
4. 1-Dodecene oxide, C₁₂H₂₄O (Fluka, 95%)
5. Cyclohexene oxide, C₆H₁₀O (Fluka, 98%)
6. Butyl-glycidyl ether, C₇H₁₄O (Fluka, 95%)
7. *tert*-Butyl-glycidyl ether, C₇H₁₄O (Fluka, 97%)
8. α -Pinene oxide, C₁₀H₁₆O (Aldrich, 97%)
9. Hexane, C₆H₁₄ (Lab-Scan, reagent grade)
10. Dichloromethane, CH₂Cl₂ (Lab-Scan, reagent grade)
11. 1,2-Dichloroethane, C₂H₄Cl₂ (Lab-Scan, reagent grade)
12. Ethyl acetate, C₄H₈O (Lab-Scan, reagent grade)
13. 1,4-Dioxane, C₄H₈O₂ (May&Baker, reagent grade)
14. Tetrahydrofuran, C₄H₈O (Lab-Scan, reagent grade)
15. *N,N'*-Dimethylformamide, C₃H₇ON (Lab-Scan, reagent grade)
16. Acetonitrile, CH₃CN (Lab-Scan, reagent grade)
17. Isooctane, C₇H₁₈Cl (Lab-Scan, reagent grade)
18. Methanol, CH₃OH (Merck, reagent grade)

19. Ethanol, C_2H_5OH (Merck, reagent grade)
20. *n*-Propanol, C_3H_7OH (Merck, reagent grade)
21. *i*-Propanol, C_3H_7OH (Merck, reagent grade)
22. *n*-Butanol, C_4H_9OH (Lab-Scan, reagent grade)
23. *tert*-Butanol, C_4H_9OH (Fluka, reagent grade)
24. Tin chloride, $SnCl_2$ (reagent grade)
25. Mercury chloride, $HgCl_2$ (reagent grade)
26. Potassium permanganate, $KMnO_4$ (Aldrich, 99+%)
27. Hydrochloric acid S.G. 37%, HCl (Fisher Chem, reagent grade)
28. Nitric acid 65%, HNO_3 (Merck, reagent grade)
29. Sulfuric acid 95-97%, H_2SO_4 (Merck, reagent grade)
30. Acetone, C_3H_6O (commercial grade)
31. Diethyl ether, $C_4H_{10}O$ (Merck, reagent grade)

3.3 Homoionic clays

Homoionic clays were prepared by purification and then ion exchange following the previous work by Kanjanaboonmalert [37].

3.3.1 Purification of Bentonite

Bentonite was purified by fractionated sedimentation. Thirty grams of bentonite were dispersed in 1,000 mL of deionized water under vigorous stirring for 3 h at room temperature. The colloid bentonite was collected and separated from quartz sediments by centrifugation. The colloid clay was centrifuged at 4,000 rpm and dried at 100°C. The purified bentonite was characterized by XRD technique.

3.3.2 Na-ion exchange

Na-clays (Na-Bentonite and Na-Hectorite) were prepared by cation exchange. Na-ion was intercalated between the clay layers. The purified bentonite or starting hectorite was suspended in 5 M NaOH with the ratio of clay to Na-solution as 1 g: 50 mL for 1 day at room temperature. Then the products were washed with deionized water until hydroxide anions were eliminated, and then the products were collected by centrifugation. The above process was repeated five times and three times for

Na-exchanged bentonite and Na-exchanged hectorite, respectively. The Na-exchanged clays were characterized using XRD technique.

3.4 Synthesis of Fe-pillared clays

Fe-pillared clays were synthesized according to Kanjanaboonmalert [37] by intercalation of iron precursors, following by calcinations at high temperature. Na-clays were dispersed in deionized water (10 %w/w) by vigorous stirring for 1 day at room temperature. Then 1 M iron (III) chloride solution, by the ratio of Fe³⁺ to clay of 10 meq per gram, was slowly added in the suspended Na-clay under stirring for 24 h at room temperature. The products were collected by centrifugation, then washed with deionized water until chloride ions were eliminated. The as-synthesized products, Fe₁₀-intercalated hectorite (as-HFe₁₀) and Fe₁₀-intercalated bentonite (as-BFe₁₀) were dried at 100°C for 1 day, followed by calcined at 300°C for 5 h in a muffle furnace. For denotation, 10 is the amount of iron loading in meq per gram of clay, B and H are bentonite and hectorite, respectively. The calcined products obtained were designated as HFe₁₀ and BFe₁₀. The obtained products were characterized using XRD technique.

3.5 Determination of acidity [38]

Acidity of raw clays and Fe-pillared clays was determined by volumetric titration. In this method, 0.2 g of the clay, previously dried at 120°C for 6 hours, was taken into a conical flask to which 15 mL of 0.1 M NaOH was added. After stirring the flask for 2 h, excess NaOH was titrated with 0.05 M H₂SO₄. Acidity was determined as milliequivalents of NaOH used per 100 g of clay.

$$\text{Acidity of clay (meq/100 g clay)} = \frac{(V1-V2) \times [H_2SO_4] \times 100}{\text{amount of clay}}$$

Where V1 is the volume of NaOH and V2 is the volume of H₂SO₄

3.6 Determination of iron content by redox titration

Iron content of samples was analyzed by Zimmermann-Reinhardt method following the recommendation of Gilbert [34].

Accurately weigh two 0.1 g samples into two 250 mL beakers. To each beaker add 8 mL of conc HCl and 2 mL of 0.25 M SnCl₂; cover with a watch glass. Heat the beakers in a hood at just below the boiling point until the samples are dissolved. Add an additional 1-2 mL of 0.25 M SnCl₂ to eliminate any yellow color that may develop during heating. If the final solution is colorless because of an excess of Sn(II), add 0.02 M KMnO₄ just to restore the yellow color. Heat the sample solution nearly to boiling and add 0.25 M SnCl₂ solution dropwise until the yellow color just disappears. Rinse down the sides of the flask with a very small amount of water and then add not more than 2 drops of excess SnCl₂.

Cool the sample to room temperature and rapidly add 10 mL of 5% HgCl₂ solution, and mix well. A small amount of a silky-white precipitate (Hg₂Cl₂) should occur.

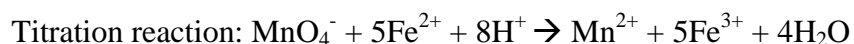
(1) If no precipitate forms, the amount of SnCl₂ is insufficient, and reduction of Fe(III) is incomplete. Discard the sample.

(2) If a gray precipitate forms, this indicates the formation of elemental mercury occur discard the sample.

Wait 2-3 min after addition of the HgCl₂ solution, then add 25 mL of Zimmermann-Reinhardt reagent and 150 mL of water. Titrate the solution immediately with the freshly standardized 0.02 M KMnO₄ solution to the first detectable pink tinge that persists for at least 30 seconds.

Determine the blank as follows: in a flask contain 8 mL conc HCl and 10 mL of water, add two drops of the SnCl₂ solution and 10 mL of 5% Hg₂Cl₂ solution. Then proceed all steps as in the determination above.

Subtract the volume used for the blank solution used from the volume for the sample. Calculate % Fe by mass in the unknown. To minimize air oxidation of Fe(II), carry out the above steps one sample at a time.



3.7 Preparation of authentic samples

2-Methoxy-2-phenylethanol [39]

Styrene oxide 1.2 mL (10 mmol) was dissolved in MeOH (30 mL) and Fe(TCA)₃·1.5 H₂O 0.0454 g (0.1 mmol) was added. The reaction mixture was stirred at room temperature for 24 h. After the reaction was finished, the crude product was extracted several times with Et₂O. The combined organic extract was washed with water and dried over anhydrous Na₂SO₄. The solution was filtered and evaporated to dryness. The residue was purified by column chromatography using hexane: EtOAc 8:2 as an eluent. The product 2-methoxy-2-phenylethanol was obtained as colorless oil. ¹H-NMR (CDCl₃) δ (ppm): 7.40-7.29 (5H, *m*), 4.34 (1H, *dd*, *J* = 3.9, 8.6 Hz), 3.71 (1H, *dd*, *J* = 8.4, 11.7), 3.64 (1H, *dd*, *J* = 3.9, 11.7 Hz) and 3.34 (3H, *s*).

2-Methoxy-1-phenylethanol [40]

To a mixture of styrene oxide 1.2 mL (10 mmol) and MeONa/MeOH in 30 mL was stirred at room temperature for 24 h. After the reaction was finished, the crude product was extracted several times with Et₂O. The combined organic extract was washed with water and dried over anhydrous Na₂SO₄. The solution was filtered and evaporated to dryness. The residue was purified by column chromatography using hexane: EtOAc 8:2 as an eluent. ¹H-NMR (CDCl₃) δ (ppm): 7.43-7.29 (5H, *m*), 4.93 (1H, *dd*, *J* = 3.9, 8.6 Hz), 3.64 (1H, *dd*, *J* = 3.8, 11.7), 3.58 (1H, *dd*, *J* = 3.1, 9.8 Hz) and 3.45 (3H, *s*).

2-Ethoxy-2-phenylethanol, 2-Propoxy-2-phenylethanol, 2-Isopropoxy-2-phenylethanol, 2-Butoxy-2-phenylethanol, 2-tert-Butoxy-2-phenylethanol

Styrene oxide 1.2 mL (10 mmol) was dissolved in 30 mL of selected alcohol (ethanol, *n*-propanol, *i*-propanol, *n*-butanol and *tert*-butanol) and Fe(TCA)₃·1.5 H₂O 0.0454 g (0.1 mmol) was added. The reaction mixture was stirred at room temperature for 24 h. After the reaction was finished, the crude product was extracted several times with Et₂O. The combined organic extract was washed with water and dried over anhydrous Na₂SO₄. The solution was filtered and evaporated to dryness. The residue was purified by column chromatography by using hexane: EtOAc as an eluent.

2-Ethoxy-2-phenylethanol: colorless liquid; $^1\text{H-NMR}$ (CDCl_3) δ (ppm): 7.36-7.26 (5H, *m*), 4.42 (1H, *dd*, $J = 3.5, 8.8$ Hz), 3.69-3.57 (2H, *m*), 3.42 (2H, *q*, $J = 7.0$ Hz) and 1.22 (3H, *t*, $J = 7.0$ Hz).

2-Propoxy-2-phenylethanol: colorless liquid; $^1\text{H-NMR}$ (CDCl_3) δ (ppm): 7.41-7.29 (5H, *m*), 4.43 (1H, *dd*, $J = 3.9, 7.8$ Hz), 3.69 (2H, *dd*, $J = 3.9, 11.6$ Hz), 3.40 (2H, *t*, $J = 6.9$ Hz), 1.65 (2H, sextet, $J = 7.2$ Hz) and 0.96 (3H, *t*, $J = 7.4$ Hz).

2-Iso-propoxy-2-phenylethanol: colorless liquid; $^1\text{H-NMR}$ (CDCl_3) δ (ppm): 7.43-7.30 (5H, *m*), 4.57 (1H, *dd*, $J = 4.5, 8.0$ Hz), 3.67-6.59 (3H, *m*), 1.23 (3H, *d*, $J = 6.2$ Hz) and 1.16 (3H, *d*, $J = 6.2$ Hz).

2-Butoxy-2-phenylethanol: colorless liquid; $^1\text{H-NMR}$ (CDCl_3) δ (ppm): 7.43-7.22 (5H, *m*), 4.47 (1H, *dd*, $J = 3.8, 8.5$ Hz), 3.79-3.68 (2H, *m*), 3.42 (2H, *t*, $J = 6.9$ Hz), 1.18-1.55 (2H, *m*), 1.40 (2H, sextet, $J = 7.2$ Hz) and 0.90 (3H, *t*, $J = 7.4$ Hz).

2-tert-Butoxy-2-phenylethanol: colorless liquid; $^1\text{H-NMR}$ (CDCl_3) δ (ppm): 7.40-7.20 (5H, *m*), 4.62 (1H, *dd*, $J = 4.4, 8.4$ Hz), 3.48 (1H, *dd*, $J = 8.4, 11.0$ Hz), 3.58 (1H, *dd*, $J = 4.4, 11.0$ Hz) and 1.22 (9H, *s*).

2-Methoxy-1-dodecanol, 1-methoxy-2-dodecanol

$\text{Fe}(\text{TCA})_3 \cdot 1.5 \text{H}_2\text{O}$ 0.0454 g (0.1 mmol) was dissolved in MeOH (30 mL), followed by the addition of 1-dodecene oxide (10 mmol) to the solution. The reaction mixture was stirred at room temperature for 24 h. After the reaction was finished, the crude product was extracted several times with Et_2O . The combined organic extract was washed with water and dried over anhydrous Na_2SO_4 . The solution was filtered and evaporated to dryness. The residue was purified by column chromatography by using hexane: EtOAc 9:1 as an eluent.

2-Methoxy-1-dodecanol: $^1\text{H-NMR}$ (CDCl_3) δ (ppm): 3.70 (1H, *dd*, $J = 2.9, 11.1$ Hz), 3.52 (1H, *dd*, $J = 6.4, 11.7$ Hz), 3.44 (3H, *s*), 3.38-3.23 (1H, *m*), 1.68-1.44 (2H, *m*), 1.40-1.22 (16H, *m*) and 0.92 (3H, *t*, $J = 6.7$ Hz).

1-Methoxy-2-dodecanol: $^1\text{H-NMR}$ (CDCl_3) δ (ppm): 3.88-3.75 (1H, *m*), 3.45 (1H, *d*, $J = 2.9$ Hz), 3.52 (1H, *t*, $J = 8.2$ Hz), 3.44 (3H, *s*), 1.48-1.44 (2H, *m*), 1.38-1.23 (16H, *m*) and 0.90 (3H, *t*, $J = 6.8$ Hz).

3-Butoxy-2-methoxy-propan-1-ol, 1-butoxy-3-methoxy-propan-2-ol, 3-tert-butoxy-2-methoxy-propan-1-ol and 1-tert-butoxy-3-methoxy-propan-2-ol.

Butyl glycidyl ether or *tert*-butyl glycidyl ether (10 mmol) was dissolved in 30 mL of MeOH and Fe(TCA)₃.1.5 H₂O 0.0454 g (0.1 mmol) was added. The reaction mixture was stirred at room temperature for 24 h. After the reaction was finished, the crude product was extracted several times with Et₂O. The combined organic extract was washed with water and dried over anhydrous Na₂SO₄. The solution was filtered and evaporated to dryness. The residue was purified by column chromatography by using hexane: EtOAc 10:1 as an eluent.

3-Butoxy-2-methoxy-propan-1-ol: ¹H-NMR (CDCl₃) δ (ppm): 3.91-3.87 (1H, *m*), 3.61-3.55 (4H, *m*), 3.51-3.45 (2H, *m*), 3.41 (3H, *s*), 1.48-1.38 (2H, *m*), 1.30-1.17 (2H, *m*) and 0.86 (3H, *t*, *J* = 7.3 Hz).

1-Butoxy-3-methoxy-propan-2-ol: ¹H-NMR (CDCl₃) δ (ppm): 4.90 (1H, *t*, *J* = 3.6 Hz), 3.72-3.69 (4H, *m*), 3.49 (1H, *t*, *J* = 3.6 Hz), 3.24 (3H, *s*), 1.46 (2H, *quin*, *J* = 7.0 Hz), 1.33 (2H, *sextet*, *J* = 7.0 Hz) and 0.96 (2H, *t*, *J* = 7.3 Hz).

3-tert-Butoxy-2-methoxy-propan-1-ol: ¹H-NMR (CDCl₃) δ (ppm): 3.80 (1H, *s*), 3.50-3.31 (4H, *m*), 3.39 (3H, *s*) and 1.20 (9H, *s*).

1-tert-Butoxy-3-methoxy-propan-2-ol: ¹H-NMR (CDCl₃) δ (ppm): 4.90 (1H, *t*, *J* = 3.6 Hz), 3.75-3.69 (4H, *m*), 3.24 (3H, *s*) and 1.21 (9H, *s*).

3.8 Optimum conditions study on styrene oxide ring opening reaction

3.8.1 General procedure

The ring opening of styrene oxide by MeOH was performed. The mixture of styrene oxide 0.12 mL (1 mmol) and MeOH (3 mL) were added to a round bottom flask with 30 wt % of catalyst to styrene oxide, connected with a condenser for refluxing. The solution was continuously stirred for desired time and temperature. After the specific time or the reaction was finished, monitored by TLC, the catalyst was simply filtered out of the mixture, and washed the product out with Et₂O. The solvent was evaporated to dryness under reduced pressure to afford the product. The product was analyzed by GC with the addition of an exact amount of an appropriate internal standard (cyclohexanone).

3.8.2 Effect of the amount of catalyst

The styrene oxide ring opening reaction was carried out according to the general procedure above, but the amount of catalyst (Fe-pillared hectorite) to styrene oxide was changed to 30 wt%, 50 wt%, 70 wt% and 100 wt%.

3.8.3 Effect of reaction time and reaction temperature

The styrene oxide ring opening reaction was performed according to the general procedure, but varied reaction time as 10 min, 30 min, 2 h, 4 h, 6 h, 24 h and reaction temperature as 30°C and 70°C.

3.8.4 Effect of solvent

The styrene oxide ring opening reaction was performed. A variety of solvents were investigated as following: hexane, CH₂Cl₂, 1,2-dichloroethane, EtOAc, 1,4-dioxane, THF, DMF, CH₃CN, isooctane.

3.8.5 Effect of the amount of nucleophile

The styrene oxide ring opening was carried out in the same manner as previously but the amount of MeOH was changed to 5, 10, 20, 30 and 50 mmol.

3.9 Effect of oxygen nucleophile for styrene oxide ring opening

According to general procedure of ring opening reaction using styrene oxide as starting material, the oxygen nucleophile was switched to different alcohols such as ethanol, *n*-propanol, *iso*-propanol, *n*-butanol and *tert*-butanol. The chosen conditions included using Fe-pillared bentonite as catalyst and CH₂Cl₂ as solvent at refluxing temperature for 2 h.

3.10 Study on other epoxides ring opening

3.10.1 1-Dodecene oxide

According to the general procedure, the ring opening reaction of 1-dodecene oxide using MeOH and Fe-pillared bentonite as nucleophile and catalyst respectively, was carried out at different reaction times (10 min, 2 and 4 h) and reaction temperatures (0°C, 30°C and 70°C).

3.10.2 Butyl glycidyl ether and *tert*-butyl glycidyl ether

The butyl glycidyl ether and *tert*-butyl glycidyl ether ring opening reactions were performed according to the general procedure using MeOH and Fe-pillared bentonite as nucleophile and catalyst, respectively. The reaction temperatures (30°C and 70°C) and reaction times (10 min, 2 and 4 h) were varied.

3.10.3 Cyclohexene oxide

The ring opening reaction of cyclohexene oxide was examined according to the general procedure using MeOH and Fe-pillared bentonite as nucleophile and catalyst, respectively at 70°C for 10 min.

3.10.4 α -Pinene oxide

According to general procedure of ring opening, the reaction using α -pinene oxide, MeOH and Fe-pillared bentonite as starting material, nucleophile and catalyst, respectively was carried out at 70°C for 10 min.

CHAPTER IV

RESULTS AND DISCUSSION

4.1 The characterization of clays

Raw clays, hectorite and bentonite, were characterized by X-ray diffraction (XRD).

4.1.1 X-ray diffraction (XRD)

The characteristic structures of raw clays were characterized by XRD technique. The analysis of the XRD patterns of raw material hectorite and bentonite are shown in Figures 4.1 and 4.2, respectively.

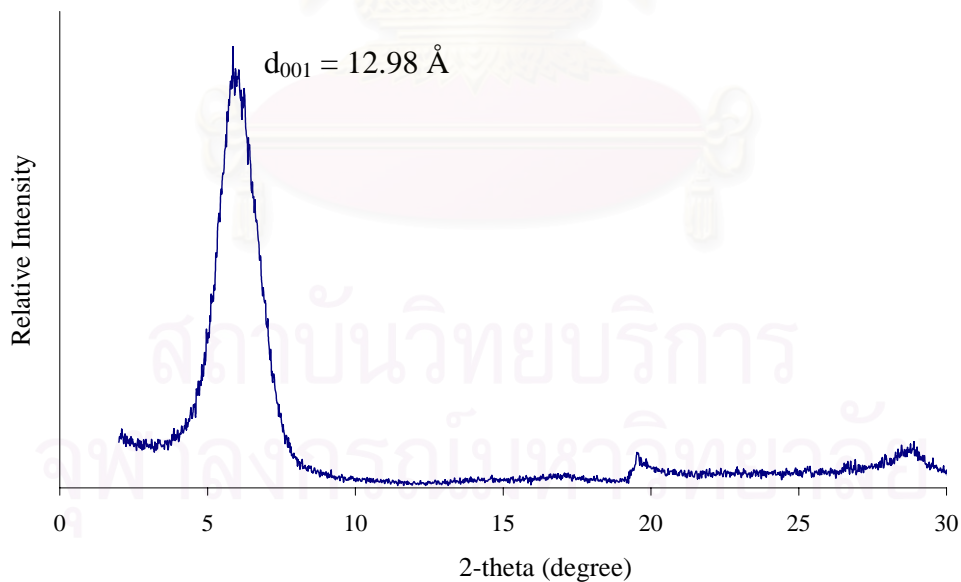


Figure 4.1 XRD pattern of raw material hectorite.

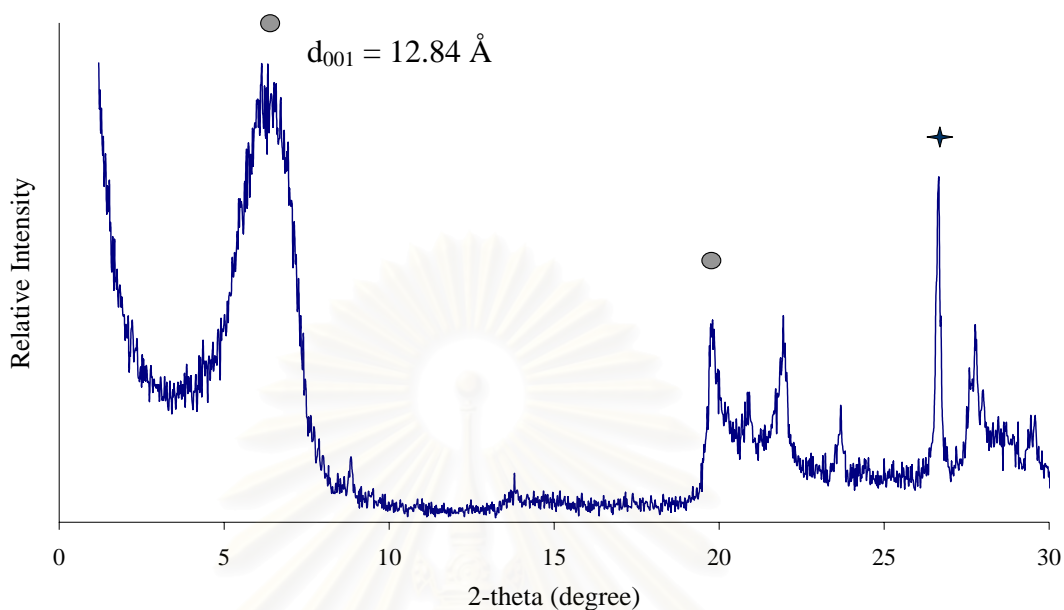


Figure 4.2 XRD pattern of raw material bentonite (● represents bentonite peaks and ✦ represents impurity quartz peak).

In Figure 4.1, raw hectorite shows the characteristic peak at 2-theta about 6.8 degree. None of other crystalline phases was presented.

In Figure 4.2, raw bentonite shows the characteristic peak at 2-theta about 7 degree. The main impurity was quartz (SiO_2), which gave the sharp peak at 26.6 degree.

4.2 The synthesis and characterization of homoionic clays

Homoionic hectorite was prepared by ion exchange method. Homoionic bentonite was purified prior to ion exchange.

4.2.1 Purification of bentonite

Raw material of bentonite contains quartz and other impurities. These impurities were removed from bentonite by dispersion and centrifugation approach. The quartz peak disappeared in purified bentonite collected from the centrifugal speed of 4000 rpm, suggesting free silica was removed from raw material bentonite. The XRD patterns of raw material bentonite and purified bentonite are shown in Figure

4.3. Purified bentonite shows the d_{001} spacing in the range of 12 to 13 Å. The XRD patterns still show the characteristic peaks of bentonite.

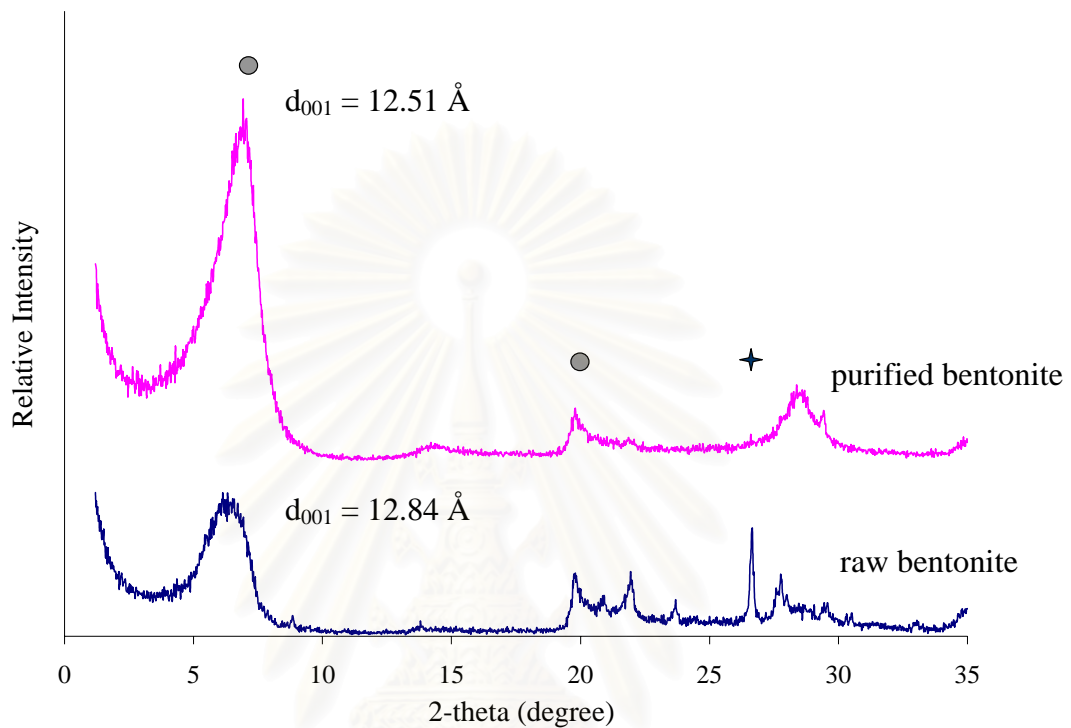


Figure 4.3 XRD patterns of raw material bentonite and purified bentonite obtained at the centrifugal speed of 4000 rpm (● represents bentonite peaks and ✦ represent impurity quart peak).

4.2.2 Na-ion exchange

4.2.2.1 X-ray diffraction of Na-hectorite

Na-ion exchange was intercalated between the clay layers. Hectorite treated with 5 M NaOH for five times was chosen as starting homoionic clay and designated as Na-hectorite. Figure 4.4 shows XRD patterns of raw material hectorite and Na-hectorite. The d_{001} spacings of Na-hectorite are higher than of the untreated one suggesting Na ions intercalate into the clay layers and NaOH does not destroy the clay layered structure. The d_{001} spacing in Na-hectorite is 15.33 Å.

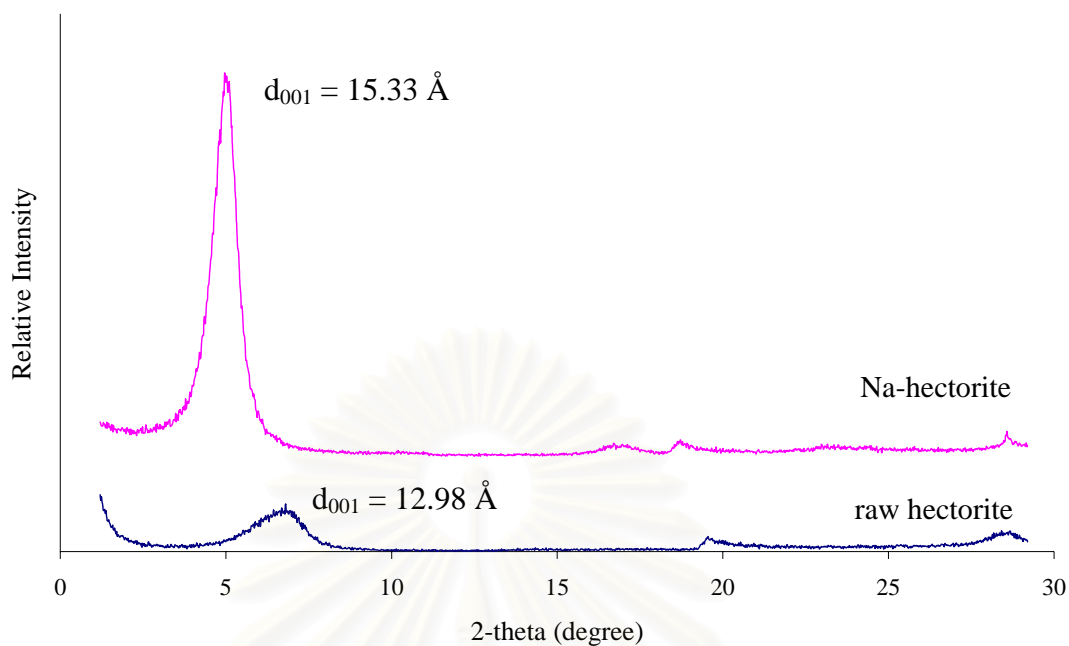


Figure 4.4 XRD patterns of raw material hectorite and Na-hectorite.

4.2.2.2 X-ray diffraction of Na-bentonite

Na-ion exchange was intercalated between the clay layers. Bentonite treated with 5 M NaOH for three times, was chosen as starting homoionic clay and designated as Na-bentonite. The XRD patterns of purified bentonite and Na-bentonite are shown in Figure 4.5. The d_{001} spacings of Na-bentonite are higher than of the untreated which suggests that Na ions intercalate into the clay layers and NaOH does not destroy the clay layered structure. The d_{001} spacing in Na-bentonite is 15.17 Å.

สถาบันวิทยบริการ
จุฬาลงกรณ์มหาวิทยาลัย

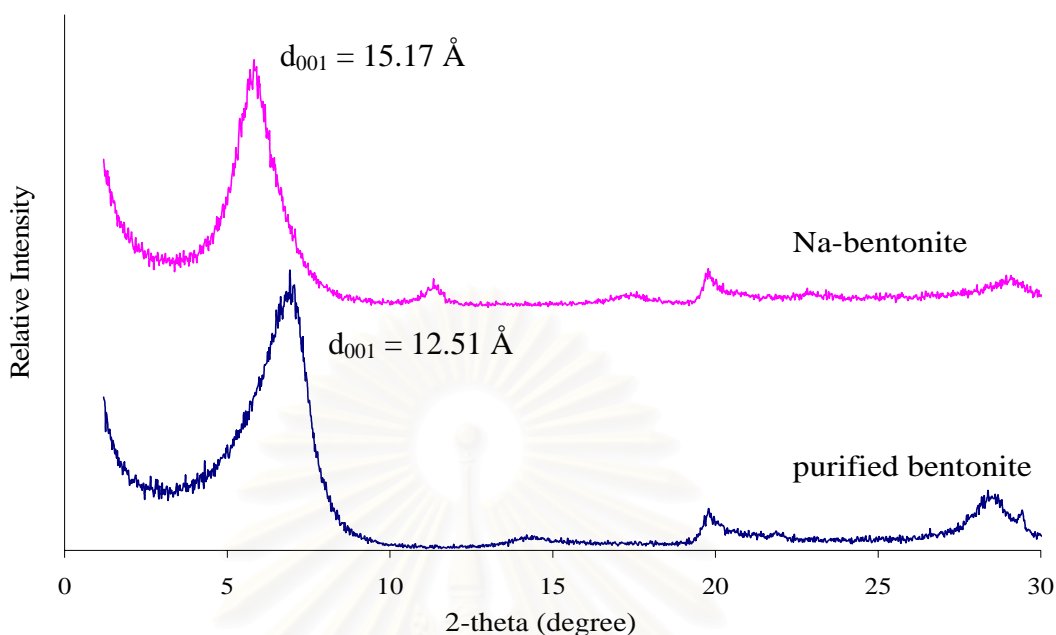


Figure 4.5 XRD patterns of purified bentonite and Na-bentonite.

4.3 The synthesis and characterization of Fe-pillared clays

According to Kanjanaboonmalert, Fe-pillared hectorite and bentonite were synthesized by intercalation of iron precursors between the clay layers, following by calcinations at high temperature. The amount of Fe in pillaring agent was 10 meq per gram of clays. All as-synthesized products [Fe₁₀-intercalated hectorite (as-HFe₁₀) and Fe₁₀-intercalated bentonite (as-BFe₁₀)] were calcined at 300°C for 5 h. Fe-pillared hectorite (HFe₁₀) and Fe-pillared bentonite (BFe₁₀) were successfully synthesized. The products are red-brown solids.

4.3.1 X-ray diffraction of Fe-precursor intercalated clay layer

The XRD patterns of raw material hectorite and as-HFe₁₀ are shown in Figure 4.6. The d_{001} reflection peak of as-HFe₁₀ was shifted from 12.98 Å to 15.23 Å. The higher d_{001} spacing of as-HFe₁₀ can be described by intercalation of iron precursor between clay layers.

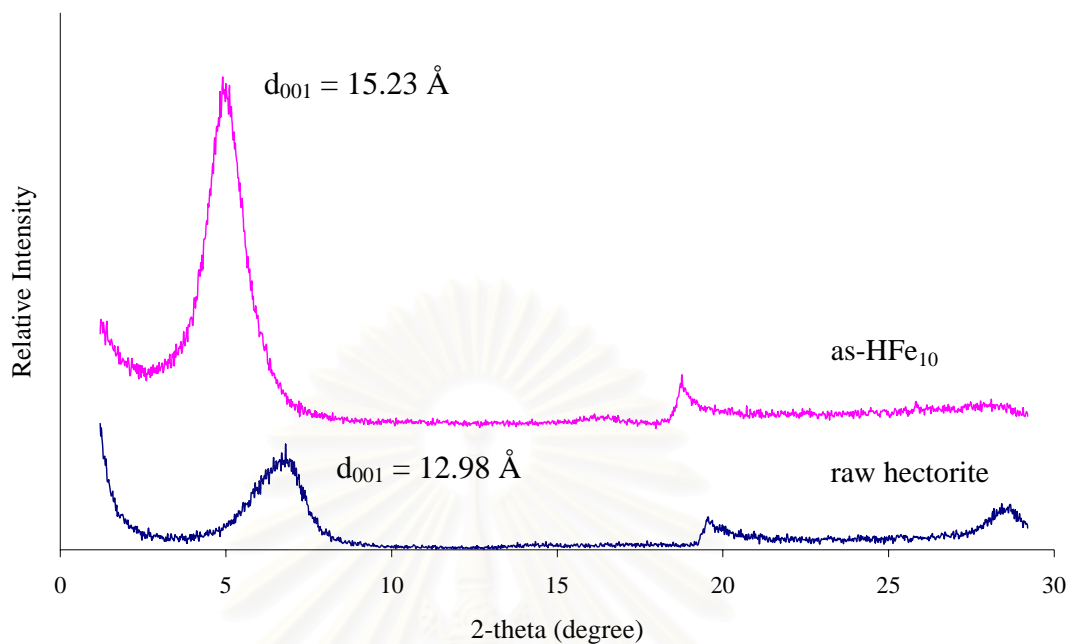


Figure 4.6 XRD patterns of raw material hectorite and Fe₁₀-intercalated hectorite (as-HFe₁₀).

4.3.2 X-ray diffraction of Fe-pillared clays

As-synthesized products (as-HFe₁₀, as-BFe₁₀) and raw clays were calcined at 300°C for 5 h. The XRD patterns of calcined raw hectorite and HFe₁₀ are shown in Figure 4.7, and the XRD patterns of calcined purified bentonite BFe₁₀ are shown in Figure 4.8. The d₀₀₁ spacing of HFe₁₀ and BFe₁₀ were lower than calcined raw hectorite and calcined purified bentonite, respectively. It can be explained that excess water molecules adsorbed between clay layers were removed and iron precursors were converted to iron oxide at calcine condition.

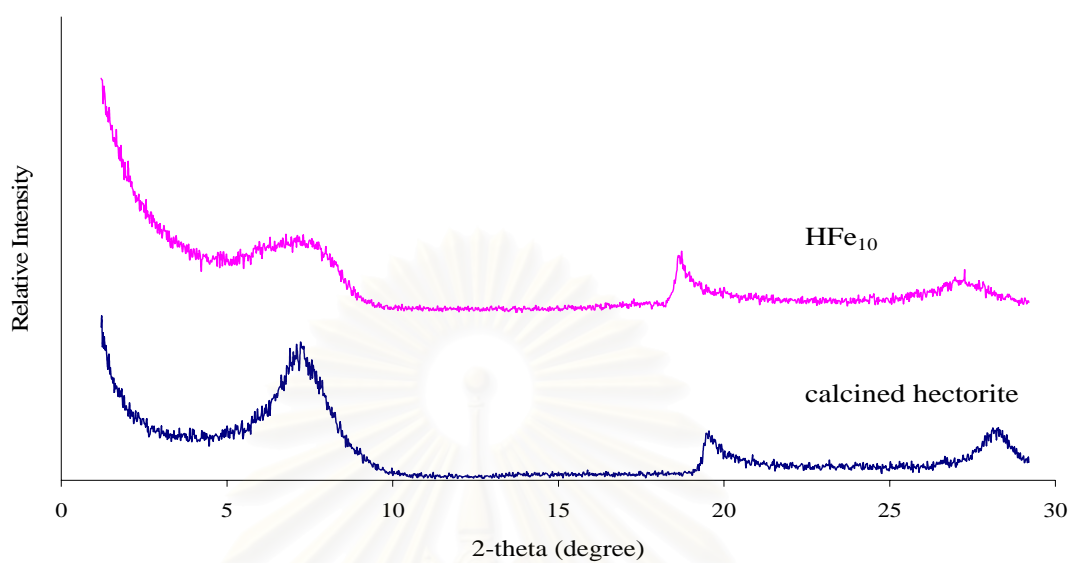


Figure 4.7 XRD patterns of calcined raw hectorite and HFe₁₀.

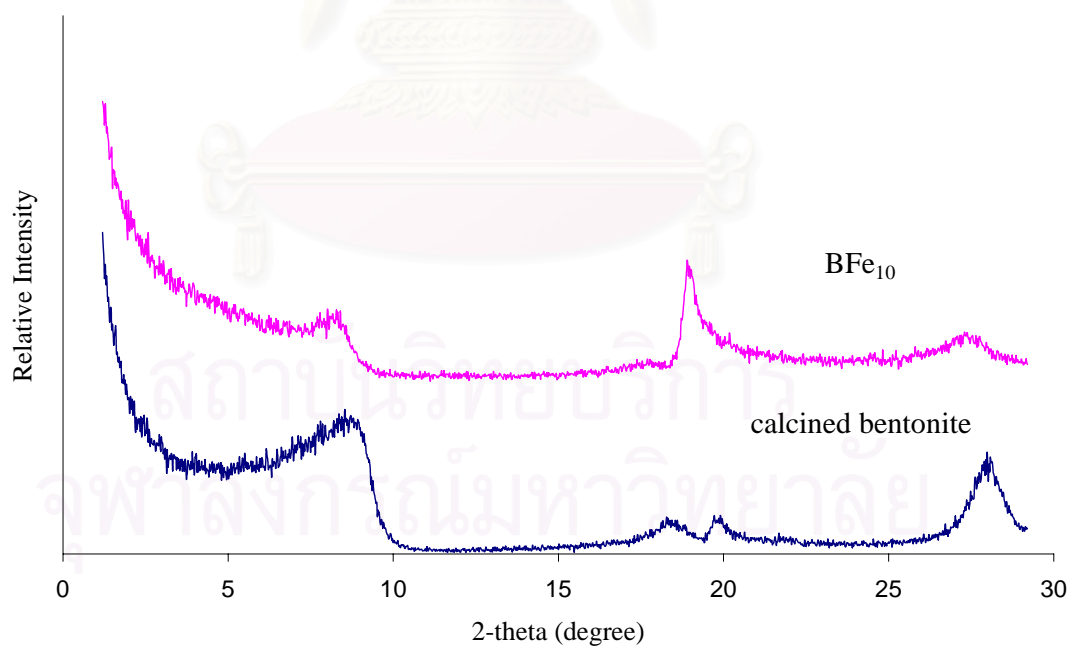


Figure 4.8 XRD patterns of calcined purified bentonite and BFe₁₀.

4.3.3 Determination of iron contents

The iron content in samples was determined by redox titration method. The results are shown in Table 4.1.

Table 4.1 The iron contents in clays and Fe-pillared clays

Samples	% Fe ₂ O ₃
Raw hectorite	1.13
Fe-pillared hectorite	21.01
Raw bentonite	4.85
Fe-pillared bentonite	29.18

The iron contents of both Fe-pillared clays are higher than those of raw clays, which can be explained that iron species can intercalate into raw clay. The iron contents of Fe-pillared bentonite are higher than that of Fe-pillared hectorite. The iron contents are depended on the source of clays.

4.3.4 Determination of acidity properties

In table 4.2, the acidity of raw clays and Fe-pillared clays determined by sodium hydroxide titration is expressed in meq of NaOH used per 100 g of clay.

Table 4.2 Acidity values of clays and Fe-pillared clays

Samples	Acidity (meq/100g of clay)
Raw hectorite	21.10
Fe-pillared hectorite	98.27
Raw bentonite	33.41
Fe-pillared bentonite	150.15
Fe ₂ O ₃	0

The acidic character of pillared clays derives from either brønsted or lewis site. Brønsted acidic appears to be associated with the coordination of water molecule with iron in pillars, while Lewis acidic is attributed to the Fe_2O_3 in pillars. The nature and strength of acid site are related to the types of clays and pillared. The pillaring process enhances the acidity in Fe-pillared clays comparison to that of the raw clays. Table 4.2 shows that the acidity of Fe-pillared clays is higher than raw clays. Fe-pillared bentonite exhibited the highest acidity (150.15 meq/100 g of clay) followed by Fe-pillared hectorite, bentonite and hectorite clay, respectively.

4.3.5 Nitrogen adsorption-desorption (Brunauer-Edmelt-Teller method, BET)

The most widely used procedure for the determination of the surface of porous material is investigated using BET analysis. The BET specific surface area of raw clays (bentonite and hectorite) and Fe-pillared clays (Fe-pillared hectorite and Fe-pillared bentonite) are shown in Table 4.3. The nitrogen adsorption-desorption isotherms of Fe-pillared clays are shown in Figures A-1 to A-2.

Table 4.3 The BET specific surface area of raw clays and Fe-pillared clays

Samples	BET specific surface area (m^2/g)
Raw hectorite	57.11
Fe-pillared hectorite	116.62
Raw bentonite	65.56
Fe-pillared bentonite	144.30
Fe_2O_3	10.13

The nitrogen adsorption-desorption isotherms of both Fe-pillared clays are shown the distorted reversible type IV isotherm, indicating that Fe_2O_3 in calcined samples converts clay-layered structure (2D structure) to mesoporous structure (3D structure). Therefore, the BET specific surface areas of Fe-pillared clays were higher than pure clays. The pore size distribution of Fe-pillared clays from BJH analysis is in the range of 50 to 70 Å, indicating the mesoporous material (diameter of 20-500 Å).

4.4 Regenerated catalyst

4.4.1 X-ray diffraction of regenerated catalyst

The XRD patterns of Fe-pillared bentonite (BFe_{10}) and regenerated Fe-pillared bentonite (regenerated BFe_{10}) are shown in Figure 4.9.

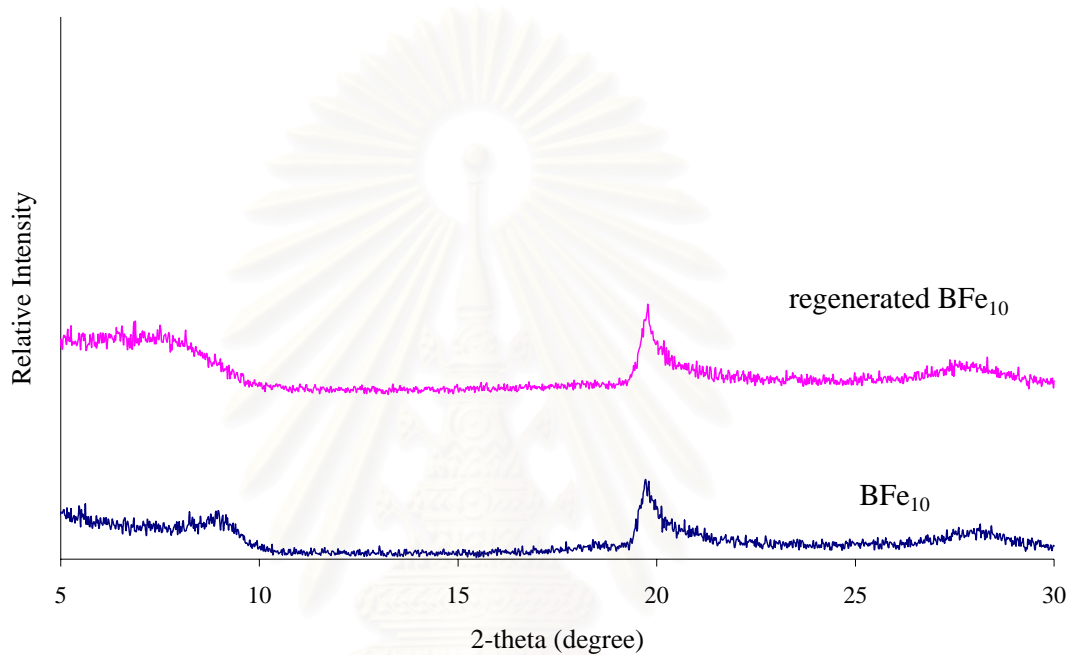


Figure 4.9 XRD patterns of BFe_{10} and regenerated BFe_{10} .

After the ring opening reaction of styrene oxide with methanol had finished, the clay catalyst was filtered from the reaction mixture and regenerated at 300°C for 5 h. The XRD pattern of regenerated BFe_{10} is similar to that of BFe_{10} .

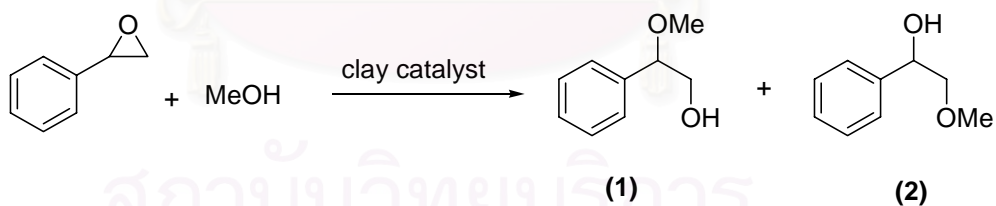
Table 4.4 The BET specific surface area of Fe-pillared bentonite and regenerated Fe-pillared bentonite

Samples	BET specific surface area (m ² /g)
Fe-pillared bentonite	144.30
Regenerated Fe-pillared bentonite	133.76

Table 4.4 shows the BET specific surface area of Fe-pillared bentonite and regenerated Fe-pillared bentonite. The BET specific surface area of regenerated catalyst decreases. It is due to the remaining organic residues in catalyst pores because the regenerated process at 300°C may not completely destroy or decompose the organic compounds adsorbed on used catalyst.

4.5 Catalytic activity of Fe-pillared clay in epoxide ring opening reaction

A ring opening reaction of styrene oxide with MeOH to produce 2-methoxy-2-phenylethanol (**1**) was selected for testing the catalytic activity of synthesized Fe-pillared clays. The reaction time, reaction temperature, the amount of catalyst, the amount of nucleophile and solvent were varied to search for the optimal conditions.



2-Methoxy-2-phenylethanol (**1**) was detected as a sole product while none of 2-methoxy-1-phenylethanol (**2**) was observed. The product was identified by GC and ¹H-NMR compared with authentic specimen synthesized. The preparation of authentic sample **1** involved the reaction of styrene oxide with MeOH using Fe(TCA)₃·1.5H₂O as a catalyst. The ¹H-NMR spectrum revealed the peak of –CH₂OH as a double doublet with 1H intensity at δ 3.71 (*J* = 8.4, 11.6 Hz) and a double doublet (1H) at δ 3.64 (*J* = 3.8, 11.6 Hz), those of aromatic protons as multiplet (5H) at δ 7.21-7.40, the peak of –OCH₃ as a singlet (3H) at δ 3.34 and that of –CHOCH₃ as a double doublet (1H) at δ 4.34 (*J* = 3.9, 8.6 Hz). The synthesis of authentic sample **2** was

performed by the reaction of styrene oxide with NaOMe in MeOH at room temperature as previously reported in literature [40]. The $^1\text{H-NMR}$ spectrum displayed the peak of $-\text{CHOH}$ as a double doublet (1H) detected at δ 4.92 ($J = 3.9, 8.6$ Hz), aromatic protons appeared as a multiplet (5H) at δ 7.21-7.40, the peak of $-\text{OCH}_3$ as a singlet (3H) at δ 3.34 and that of $-\text{CH}_2\text{OCH}_3$ as a double doublet (1H) at δ 3.64 ($J = 3.8, 11.6$ Hz) and a double doublet (1H) at δ 3.58 ($J = 3.0, 9.7$ Hz).

Other substrates utilized in order to examine the scope of the catalytic activity of ring opening reaction of epoxides included 1-dodecene oxide, cyclohexene oxide, butyl glycidyl ether, *tert*-butyl glycidyl ether and α -pinene oxide.

4.5.1 Effect of raw clays (hectorite and bentonite) and Fe-pillared clay catalysts on the reactivity of styrene oxide ring opening

The catalytic activity of Fe-pillared clays (Fe-pillared hectorite and Fe-pillared bentonite) was compared with iron oxide (Fe_2O_3 , hematite), pure hectorite and pure bentonite. Condition for this reaction was 30 wt% catalyst to styrene oxide at 70°C for 24 h. The results are shown in Table 4.5. Both Fe-pillared clays gave much higher % yield than pure clays and Fe_2O_3 .

Table 4.5 Effect of raw clays (hectorite, bentonite clays) and Fe-pillared clays catalyst on the reactivity of styrene oxide ring opening

Catalyst	% yield of 1 (based on substrate)	% styrene oxide (recovered)	MB
None	0	93.39	93.39
Raw hectorite	2.29	95.45	97.74
Raw bentonite	3.12	91.23	94.35
Fe_2O_3	21.24	74.50	95.74
Fe-pillared hectorite	64.97	24.35	89.32
Fe-pillared bentonite	103.69	0.00	103.69

Reaction condition: styrene oxide (1 mmol), MeOH (3 mL), 30 wt% catalyst to styrene oxide at 70°C for 24 h

When the reaction was performed without catalyst, no product was observed. Thus, the catalyst is needed for this reaction. In Table 4.5, raw clays and Fe₂O₃ show the lower activity than Fe-pillared clays. This result corresponds with the titration experiment to determine iron content and acidity, and nitrogen adsorption-desorption experiment to observe surface area. Fe-pillared bentonite has the highest iron content, acidity and BET surface area. Therefore it shows the most activity in ring opening reaction of styrene oxide and methanol to furnish 2-methoxy-2-phenylethanol (**1**) in high yield with excellent regioselectivity. This outcome may involve the electronic effect that stabilizes benzylic cation and may favourably induce the nucleophilic attack at this position of styrene oxide.

4.5.2 Study on the optimum conditions for styrene oxide ring opening by Fe-pillared hectorite clay

Because of the easier preparation of Fe-pillared hectorite than Fe-pillared bentonite, Fe-pillared hectorite clay was selected to use as a catalyst for styrene oxide ring opening reaction at first. The effect of reaction time and the amount of catalyst on the outcome of the reaction was examined for the optimal condition.

4.5.2.1 Effect of the reaction time on styrene oxide ring opening reaction

The effect of the reaction time on styrene oxide ring opening catalyzed by Fe-pillared hectorite was examined. The results are shown in Table 4.6.

Table 4.6 Effect of the reaction time on styrene oxide ring opening reaction catalyzed by Fe-pillared hectorite

entry	time	% yield of 1 (based on substrate)	% styrene oxide (recovered)	MB
1	10 min	45.11	51.63	96.74
2	30 min	47.92	40.60	88.52
3	2 h	49.79	47.06	96.85
4	4 h	50.22	42.05	92.27
5	24 h	64.97	24.98	89.95

Reaction condition: styrene oxide (1 mmol), MeOH (3 mL), 30 wt% Fe-pillared hectorite to styrene oxide at 70°C

The results from this table demonstrate that the ring opening reaction of styrene oxide at 70°C catalyzed by Fe-pillared hectorite (HFe₁₀) yielded **1** as a single product. The amount of the obtained product was slightly increased when reaction time increased. About 65% of product was obtained when the reaction was performed for 24 h.

4.5.2.2 Effect of the amount of catalyst on styrene oxide ring opening reaction

The amount of catalyst normally influenced the performance of the reaction. The variation of the amount of Fe-pillared hectorite on styrene oxide ring opening reaction was carried out and the results are presented in Table 4.7.

Table 4.7 Effect of the amount of Fe-pillared hectorite on styrene oxide ring opening reaction

entry	Fe-pillared hectorite	% yield of 1 (based on substrate)	% styrene oxide (recovered)	MB
1	30 wt%	45.11	51.63	96.74
2	50 wt%	71.88	18.50	90.38
3	70 wt%	75.26	19.04	94.30
4	100 wt%	88.38	4.55	92.93

Reaction condition: styrene oxide (1 mmol), MeOH (3 mL), Fe-pillared hectorite varied at 70°C for 10 min

According to the results from this table, the amount of catalyst increased the yield of the product derived from ring opening reaction of styrene oxide at 70°C. It should be mentioned here that the quantitative yield of **1** was achieved when 100 wt% of Fe-pillared hectorite to styrene oxide was employed and the reaction was conducted for 24 h.

4.5.3 Study on the optimum conditions for styrene oxide ring opening by Fe-pillared bentonite

4.5.3.1 Effect of reaction time and reaction temperature for Fe-pillared bentonite catalyzed on styrene oxide ring opening

The effect of reaction time and reaction temperature on styrene oxide ring opening was examined. The results are tabulated in Table 4.8.

Table 4.8 Effect of reaction time and reaction temperature on styrene oxide ring opening catalyzed by Fe-pillared bentonite

entry	time	at room temperature (30°C)			at 70°C		
		% yield of 1	% styrene oxide (recovered)	MB	% yield of 1	% styrene oxide (recovered)	MB
1	10 min	67.49	28.61	96.10	95.00	1.53	96.53
2	30 min	68.67	22.35	91.02	95.12	1.65	97.67
3	2 h	85.93	14.96	100.89	97.47	0	97.47
4	6 h	88.64	15.01	103.65	-	-	-

Reaction conditions: styrene oxide (1 mmol), MeOH (3 mL), 30 wt% Fe-pillared bentonite to styrene oxide

Table 4.8 reveals that the ring opening reaction of styrene oxide could be carried out at room temperature (30°C) by Fe-pillared bentonite furnishing the target product 67% within 10 min. The yield of **1** could be increased when the reaction time increased and reached 86% yield using 30 wt% Fe-pillared bentonite to styrene oxide within 2 h. Much better yield could be accomplished when the reaction temperature at 70°C was utilized, the reaction gave excellent yield within 10 min.

4.5.4 Comparison of the effect of Fe-pillared bentonite and Fe-pillared hectorite on styrene oxide ring opening

The comparative study on the effect of catalysts (Fe-pillared hectorite and Fe-pillared bentonite) on the rate of styrene oxide ring opening reaction can be summarized in Table 4.9.

Table 4.9 Comparative study on the effect of Fe-pillared hectorite and Fe-pillared bentonite on styrene oxide ring opening

entry	time	% yield of 1	
		using Fe-pillared bentonite	using Fe-pillared hectorite
1	10 min	95.00	45.11
2	30 min	95.12	47.92
3	2 h	97.47	49.79
4	24 h	-	64.97

Reaction conditions: styrene oxide (1 mmol), 30 wt% catalyst to epoxide, MeOH (3 mL) at 70°C

The comparative study on the effect of the reaction time of two catalysts Fe-pillared hectorite and Fe-pillared bentonite on styrene oxide ring opening at 70°C by 30 wt% catalyst to styrene oxide was conducted. It was observed that Fe-pillared bentonite was more efficient catalyst than Fe-pillared hectorite in the styrene oxide ring opening reaction. The yield of **1**, catalyzed by Fe-pillared bentonite was obtained more than that by Fe-pillared hectorite at all reaction time. From catalytic results of Fe-pillared hectorite and Fe-pillared bentonite, it can be concluded that type of clays (hectorite and bentonite) affects the catalytic activity in this reaction. Therefore the following study will concentrate on Fe-pillared bentonite as a catalyst in epoxide ring opening reaction.

4.5.5 Effect of the amount of nucleophile on styrene oxide ring opening catalyzed by Fe-pillared bentonite

The variation of the amount of nucleophile was examined since some nucleophiles have high cost and toxic. Thus they should be avoided employing as a

solvent. The aim of this study was to try to minimize the amount of nucleophile while maintaining the efficiency of the reaction: CH_2Cl_2 was chosen as a reaction medium. The effect of the variation of the amount of MeOH on styrene oxide ring opening catalyzed by Fe-pillared bentonite was examined and the results are presented in Table 4.10.

Table 4.10 Effect of the amount of MeOH on styrene oxide ring opening catalyzed by Fe-pillared bentonite

entry	MeOH (mmol)	% yield of 1 (based on substrate)	% styrene oxide (recovered)	MB
1	10	65.70	26.60	91.61
2	20	82.92	17.65	100.57
3	30	83.05	7.58	90.63
4	50	89.91	8.88	98.79

Reaction conditions: styrene oxide (1 mmol), 30 wt% Fe-pillared bentonite to styrene oxide, CH_2Cl_2 (3 mL), MeOH (varied) at refluxing temperature for 2 h

From Table 4.10, the yield of **1** which was derived from the ring opening reaction of styrene oxide at 40°C for 2 h using Fe-pillared bentonite as catalyst was increased when the amount of MeOH increased. The yield of **1** was quite constant when the amount of MeOH was used more than 20 mmol. Thus in the research work, the amount of MeOH 20 mmol was chosen for studying the optimum conditions of this reaction.

4.5.6 Effect of solvent on styrene oxide ring opening reaction

4.5.6.1 Effect of solvent on the styrene oxide ring opening reaction catalyzed by Fe-pillared bentonite

To observe the effect of various solvents on styrene oxide ring opening, the solvent investigated included hexane, CH_2Cl_2 , 1,2-dichloroethane, THF, EtOAc, 1,4-dioxane, CH_3CN , DMF and isooctane. The results are presented in Table 4.11.

Table 4.11 Effect of solvent on styrene oxide ring opening

Entry	solvent	% yield of 1 (based on substrate)	% styrene oxide (recovered)	MB
1	hexane	71.05	22.98	94.03
2	CH ₂ Cl ₂	82.92	17.65	100.57
3	1,2-dichloroethane	71.59	25.89	97.48
4	THF	59.78	39.56	99.34
5	EtOAc	54.92	32.58	87.50
6	1,4-dioxane	78.66	14.13	92.79
7	CH ₃ CN	38.72	53.23	91.95
8	DMF	0	87.32	87.32
9	isooctane	76.58	14.53	91.11
10	CH ₂ Cl ₂ : hexane (70 : 30)	87.06	8.75	96.01
11	CH ₂ Cl ₂ : hexane (30 : 70)	83.83	6.52	90.35

Reaction conditions: styrene oxide (1 mmol), 30 wt% Fe-pillared bentonite to styrene oxide, MeOH (20 mmol), solvent (3 mL), at refluxing temperature for 2 h

The results derived from Table 4.11, CH₂Cl₂ provided the highest yield of **1**. On the contrary, DMF was not a proper solvent for styrene oxide ring opening because of its high polarity. The more polar molecule, the stronger coordination with carbocationic intermediate. Therefore, the nucleophile (MeOH) could not attack at that carbocation. It was noticed that under these particular conditions, aprotic polar solvent was suitable for this reaction. It thus initially avoided protic solvents due to the potential complication of specific acid catalysts. The mixed solvent of hexane and CH₂Cl₂ was applied in the following experiments. It was found that the ratio of CH₂Cl₂: hexane as 70:30 was also suitable for this reaction. The yield of **1** was found to be depended on type of solvent. Nevertheless, in this research, CH₂Cl₂ was chosen as a solvent for studying the optimum conditions for epoxide ring opening reaction.

4.5.6.2 Effect of solvent and reaction time on the styrene oxide ring opening catalyzed by Fe-pillared bentonite

The effect of solvent and reaction time on styrene oxide ring opening was analyzed. The results are shown in Table 4.12.

Table 4.12 Effect of solvent and reaction time on styrene oxide ring opening catalyzed by Fe-pillared bentonite

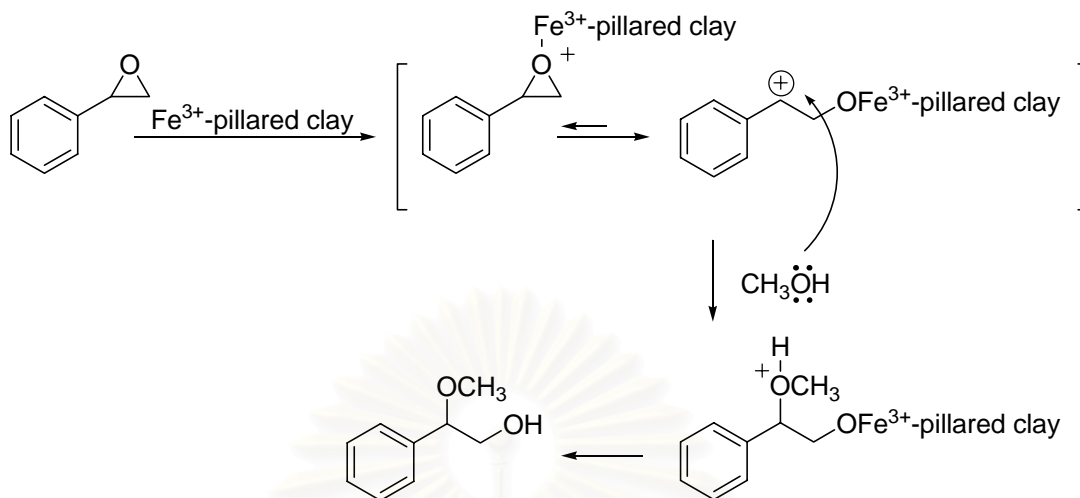
Entry	solvent	time	% yield of 1 (based on substrate)	% styrene oxide (recovered)	MB
1	CH ₂ Cl ₂	2 h	82.92	17.65	100.57
2	CH ₂ Cl ₂	5 h	94.06	5.82	99.77
3	CH ₂ Cl ₂	9 h	97.04	3.90	100.94
4	hexane	2 h	71.05	22.98	94.03
5	hexane	5 h	86.01	12.34	98.35
6	hexane	9 h	90.72	3.99	94.71

Reaction conditions: styrene oxide (1 mmol), 30 wt% Fe-pillared bentonite to styrene oxide, MeOH (20 mmol), solvent (3 mL), at refluxing temperature

The yield of **1** obtained from the reaction using CH₂Cl₂ as solvent was higher than that using hexane in all reaction times and the more time spending for the reaction, the higher yields were obtained.

It could be summarized the standard conditions for styrene oxide ring opening with MeOH catalyzed by Fe-pillared bentonite as follows: styrene oxide 1 mmol, MeOH 3 mL, 30 wt% Fe-pillared bentonite to styrene oxide, reaction temperature at 70°C and reaction time for 10 min.

The proposed mechanism of styrene oxide ring opening with MeOH in the presence of Fe³⁺-pillared clay can be depicted as shown in Scheme 4.1. It involves the coordination of the epoxide oxygen with the Fe³⁺-pillared clay which induces carbocation character of the epoxide ring carbon and the resonance effect of phenyl ring helps accumulation of the positive charge at the benzylic carbon. Then nucleophile attacks at the carbocation position to give the product.



Scheme 4.1 Proposed mechanism of styrene oxide ring opening reaction.

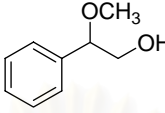
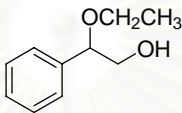
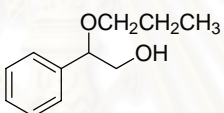
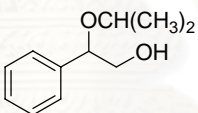
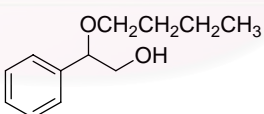
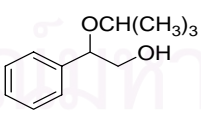
4.5.7 Variation of nucleophile for epoxide ring opening reaction

The variation of nucleophiles for styrene oxide ring opening could transform epoxide into other important products in organic chemistry. In this research, various alcohols acted as oxygen nucleophile for styrene oxide ring opening was examined.

Besides the single isomer of 2-methoxy-2-phenylethanol (**1**) was achieved when MeOH was selected as a nucleophile as previously reported, others alcohols such as ethanol, *n*-propanol, *iso*-propanol, *n*-butanol and *tert*-butanol were used to observe the scope of this styrene oxide ring opening reaction. The results are presented in Table 4.13.

สถาบันวิทยบริการ
จุฬาลงกรณ์มหาวิทยาลัย

Table 4.13 Variation of alcohols in styrene oxide ring opening

Entry	nucleophile	% yield of product (based on substrate)	% styrene oxide (recovered)	MB
1	methanol	 82.92	17.65	100.57
2	ethanol	 76.30	19.56	95.86
3	<i>n</i> -propanol	 64.24	26.09	90.33
4	<i>iso</i> -propanol	 70.80	25.5	96.30
5	<i>n</i> -butanol	 55.90	39.45	95.35
6	<i>tert</i> -butanol	 49.44	40.56	90.00

Reaction conditions: styrene oxide (1 mmol), alcohol (20 mmol), CH₂Cl₂ (3 ml),
30 wt% Fe-pillared bentonite to styrene, at 40°C for 2 h

Table 4.13 reveals that styrene oxide could react with various alcohols using Fe-pillared bentonite to furnish the desired products with different extents of yield. The use of ethanol, *n*-propanol, *iso*-propanol, *n*-butanol and *tert*-butanol produced the corresponding products in lower yield than methanol nucleophile. This was no doubt to stem from the steric hindrance of bulky nucleophile to attack the electrophilic site of the molecule [41].

The structures of all products obtained were fully characterized by $^1\text{H-NMR}$ spectroscopy. To illustrate this, the peak $-\text{CHOEt}$ of 2-ethoxy-2-phenylethanol was detected as a double doublet (1H) at δ 4.42 ($J = 3.5, 8.8$ Hz), those of the $-\text{CH}_2\text{OH}$ as a multiplet (2H) at δ 3.57-3.69, that of $-\text{OCH}_2\text{CH}_3$ as a quartet (2H) at δ 3.42 ($J = 7.0$ Hz), the peak of $-\text{CH}_2\text{CH}_3$ as a triplet (3H) at δ 1.22 ($J = 7.0$ Hz) and aromatic protons as a multiplet (5H) at δ 7.26-7.36.

The $^1\text{H-NMR}$ spectrum of 2-propoxy-2-phenylethanol clearly revealed the presence of aromatic protons as a multiplet (5H) at δ 7.41-7.29. The peak of $-\text{CHCH}_2\text{OH}$ as a double doublet (1H) at δ 4.43 ($J = 3.9, 7.8$ Hz), those of the $-\text{CHCH}_{2\text{A}}\text{OH}$ as a double doublet (1H) at δ 3.70 ($J = 7.8, 11.6$ Hz) and $-\text{CHCH}_{2\text{B}}\text{OH}$ as a double doublet (1H) at δ 3.60 ($J = 3.8, 11.6$ Hz), $-\text{OCH}_2\text{CH}_2$ as a multiplet (2H) at δ 3.42-3.28, $-\text{CH}_2\text{CH}_2\text{CH}_3$ as a sextet (2H) at δ 1.65 ($J = 7.2$ Hz) and $-\text{CH}_2\text{CH}_3$ as a triplet (3H) at δ 0.96 ($J = 7.4$ Hz) were detected.

The $^1\text{H-NMR}$ spectrum of 2-*iso*-propoxy-2-phenylethanol exhibited the peaks of aromatic as a multiplet (5H) at δ 7.30-7.42, that of $-\text{CH}(\text{O}i\text{-Pr})$ as a double doublet (1H) at δ 4.57 ($J = 4.5, 8.0$ Hz), those of $-\text{CH}_2\text{OH}$ and $-\text{OCH}(\text{CH}_3)_2$ as a multiplet (3H) at δ 3.57-3.67, and those of the $-\text{OCH}(\text{CH}_3)_2$ as a doublet (3H) at δ 1.23 ($J = 6.0$ Hz) and a doublet (3H) at δ 1.16 ($J = 6.2$ Hz), respectively.

The characterization of 2-butoxy-2-phenylethanol by $^1\text{H-NMR}$ spectrum was found the peak of aromatic as a multiplet (5H) at δ 7.25-7.39. The peak of $-\text{CHCH}_2\text{OH}$ as a double doublet (1H) at δ 4.42 ($J = 3.8, 8.5$ Hz), those of the $-\text{CHCH}_2\text{OH}$ as a multiplet (2H) at δ 3.57-3.78, those of $-\text{OCH}_{2\text{A}}\text{CH}_2$ as a doublet of triplet (1H) at δ 3.42 ($J = 6.9, 9.3$ Hz) and $-\text{OCH}_{2\text{B}}\text{CH}_2$ as a doublet of triplet (1H) at δ 3.37 ($J = 6.9, 9.3$ Hz), the peaks of $-\text{OCH}_2\text{CH}_2\text{CH}_2\text{CH}_3$ as a multiplet (2H) at δ 1.56-1.63, those of the $-\text{OCH}_2\text{CH}_2\text{CH}_2\text{CH}_3$ as a multiplet (2H) at δ 1.35-1.42 and those of $-\text{OCH}_2\text{CH}_2\text{CH}_2\text{CH}_3$ as a triplet (3H) at δ 0.93 ($J = 7.4$ Hz).

The $^1\text{H-NMR}$ spectrum of 2-*tert*-butoxy-2-phenylethanol clearly revealed the presence of aromatic protons as a multiplet (5H) at δ 7.25-7.40. The peak of $-\text{CHOCH}(\text{CH}_3)_3$ as a double doublet (1H) at δ 4.62 ($J = 4.4, 8.4$ Hz), $-\text{CH}_{2\text{A}}\text{OH}$ as a doublet of doublet (1H) at δ 3.48 ($J = 8.4, 11.0$ Hz) and $-\text{CH}_{2\text{B}}\text{OH}$ as a doublet of doublet (1H) at δ 3.58 ($J = 4.4, 11.0$ Hz), and those of $-\text{OC}(\text{CH}_3)_3$ as a singlet (9H) at δ 1.22.

4.5.8 The ring opening of other epoxides catalyzed by Fe-pillared bentonite

Various epoxides such as 1-dodecene oxide, cyclohexene oxide, butyl glycidyl ether, *tert*-butyl glycidyl ether and α -pinene oxide were chosen to observe the action of Fe-pillared bentonite as a catalyst on epoxide ring opening reaction.

4.5.8.1 Ring opening of 1-dodecene oxide

1-Dodecene oxide was chosen as a representation of terminal aliphatic epoxide. The effect of reaction time, temperature and solvent on ring opening of 1-dodecene oxide is presented in Table 4.14.

Table 4.14 1-Dodecene oxide ring opening catalyzed by Fe-pillared bentonite

Entry	time	temp ($^{\circ}\text{C}$)	solvent	% yield of		% 1-dodecene oxide (recovered)	selectivity 3:4
				3	4		
1	10 min	0	none	3.49	2.05	98.32	1.70
2	2 h	0	none	5.83	3.51	94.31	1.66
3	10 min	70	none	60.86	40.15	3.77	1.52
4	2 h	30	none	23.36	15.46	60.45	1.51
5	2 h	40	none	58.50	38.41	0	1.52
6	2 h	40	CH_2Cl_2	63.02	40.35	0	1.56

Reaction conditions: 1-dodecene oxide (1 mmol), MeOH (3 mL), solvent (3 mL), 30 wt% Fe-pillared bentonite to styrene oxide

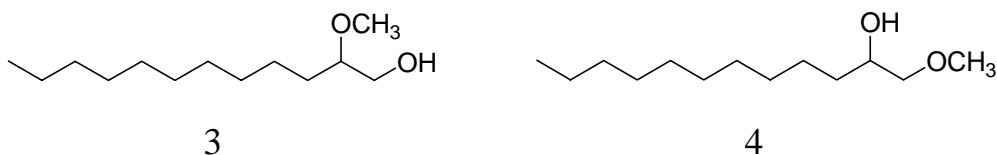


Table 4.14 shows that 1-dodecene oxide ring opening could be performed using Fe-pillared bentonite to furnish 2-methoxy-1-dodecanol (**3**) and 1-methoxy-2-dodecanol (**4**). The reaction at 70°C for 10 min (entry 3) yielded of **3** and **4** approximately 1.52:1 in 60.86% of **3** and 40.15% of **4**.

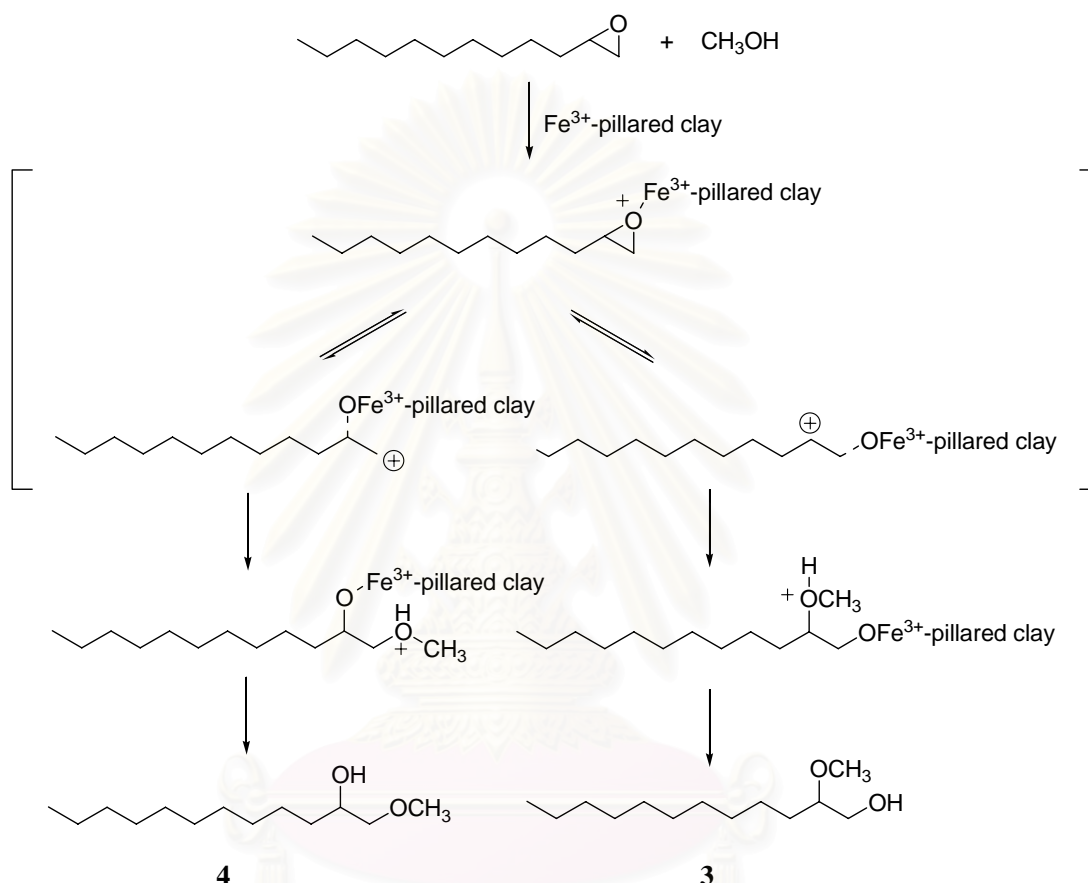
When the temperature was reduced to 0°C (entries 1-2), the total yield was less than that of standard condition (entry 3). The selectivity was however not significantly different when the reaction took place at higher temperature.

The use of CH₂Cl₂ as a reaction medium (entry 6) on 1-dodecene oxide ring opening reaction at refluxing temperature (40°C) did not increase the ratio of **3** and **4** (entry 5); nonetheless the higher yield of **3** and **4** was obtained. In summary, temperature, reaction time and solvent did not affect on the selectivity, but did affect on the reaction yield.

Two isomeric products were separated by silica gel column chromatography and characterized by ¹H-NMR spectroscopy. To illustrate this, 2-methoxy-1-dodecanol (**3**) exhibited the methylene protons belonging to -CH₂OH as a double doublet at δ 3.70 (1H, *J* = 2.9, 11.1 Hz) and δ 3.52 (1H, *J* = 6.4, 11.7 Hz), the signal of -OCH₃ as a singlet (3H) at δ 3.44, of -CHOCH₃ as a multiplet (1H) at δ 3.23-3.38, -CH₂CH(OCH₃) as a multiplet (2H) at δ 1.44-1.68, of -(CH₂)₈ as a multiplet (16H) at δ 1.22-1.40 and of -CH₃ as a triplet (3H) at δ 0.92 (*J* = 6.7 Hz). The ¹H-NMR spectrum of 1-methoxy-2-dodecanol (**4**) displayed the signal of -CH(OCH₃) as a multiplet (1H) at δ 3.75-3.88, -CH₂OH as a doublet (1H) at δ 3.45 (*J* = 2.9 Hz) and triplet (1H) at δ 3.52 (*J* = 8.2 Hz), -OCH₃ as a singlet (3H) at δ 3.44, -CH₂CH(OCH₃) as a multiplet (2H) at δ 1.44-1.48, -(CH₂)₈ as a multiplet (16H) at δ 1.23-1.38 and -CH₃ as a triplet (3H) at δ 0.90 (*J* = 6.8 Hz).

The mechanism of 1-dodecene oxide ring opening reaction with MeOH in the presence of Fe³⁺-pillared clay could propose in Scheme 4.2. The first step was the coordination of Fe³⁺-pillared clay at oxygen of epoxide ring. The nucleophile was

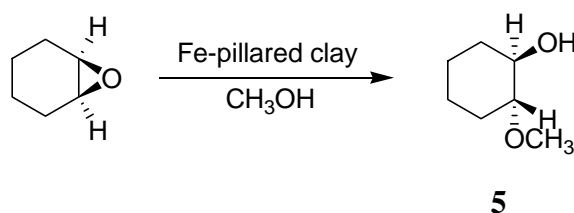
able to attack at both positions, so the two intermediates were proposed. The stability of carbocation formed was more pronounced than the steric effect, consequently **3** was obtained in higher yield than **4**.



Scheme 4.2 Proposed mechanism of 1-dodecene oxide ring opening reaction

4.5.8.2 Ring opening of cyclohexene oxide

Cyclohexene oxide was chosen as a representative of cyclic epoxide. The ring opening reaction of cyclohexene oxide could be carried out at 70°C for 10 min using 30 wt% Fe-pillared bentonite to furnish *trans*-2-methoxy-cyclohexanol (**5**) with quantitative yield and excellent regioselectivity. The reaction was proceeded with complete inversion of configuration.



The isolated product was identified by $^1\text{H-NMR}$ spectroscopy. The characterization of *trans*-2-methoxy-cyclohexanol (**5**) by $^1\text{H-NMR}$ spectrum could be accomplished by the detection of $-\text{OCH}_3$ as a singlet (3H) at δ 3.35 and the signal of $-\text{CHOH}$ as a multiplet (1H) at δ 3.32-3.41. The peak of $-\text{CHOCH}_3$ as a double doublet of doublet (1H) at δ 2.85-2.93 ($J = 4.4, 8.8, 11.2$ Hz). The peak of $-\text{CH}_2\text{CHOH}$ as a multiplet (2H) at δ 1.88-2.12 and those of $-\text{CH}_2\text{CHOCH}_3$ as a multiplet (2H) at δ 1.60-1.72. The peak of $-\text{CH}_2\text{CH}_2\text{CH}_2\text{CH}_2-$ as a multiplet (4H) at δ 1.10-1.29 and a multiplet (1H) at δ 0.97-1.08.

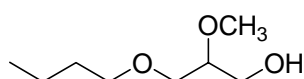
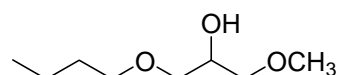
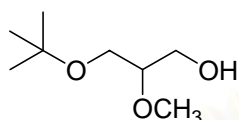
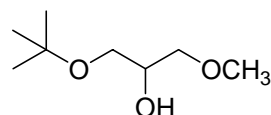
4.5.8.3 Ring opening of butyl glycidyl ether and *tert*-butyl glycidyl ether

Butyl glycidyl ether and *tert*-butyl glycidyl ether are epoxides containing an ether functional group. The effect of reaction time and temperature on butyl glycidyl ether and *tert*-butyl glycidyl ether ring opening catalyzed by Fe-pillared bentonite were examined. The results are tabulated in Tables 4.15.

Table 4.15 Butyl glycidyl ether and *tert*-butyl glycidyl ether ring opening catalyzed by Fe-pillared bentonite

Entry	time	temp (°C)	% yield of product				selectivity	
			butyl glycidyl ether		<i>tert</i> -butyl glycidyl ether		6:7	8:9
			6	7	8	9		
1	10 min	70	52.64	21.83	57.06	14.09	2.41	4.05
2	2 h	70	59.31	23.01	-	-	2.58	-
3	4 h	70	68.06	26.07	-	-	2.61	-
4	4 h	30	20.34	5.88	-	-	3.46	-
5	24 h	30	44.60	11.71	-	-	3.81	-

Reaction conditions: butyl glycidyl ether or *tert*-butyl glycidyl ether (1 mmol), MeOH (3 mL), 30 wt% Fe-pillared bentonite to styrene oxide

**6****7****8****9**

According to the results from Table 4.15, the ring opening reaction of butyl glycidyl ether and *tert*-butyl glycidyl ether could be performed using Fe-pillared bentonite as a catalyst. The yield of **6** was higher than that of **7** in all reaction conditions. At 70°C, the more yield was obtained with longer reaction time, but the selectivity was not significantly increased. The reaction was completed within 4 h. The yield of this reaction at 30°C (entry 4) was lower than that at 70°C (entry 3), but the selectivity was not significantly increased. Comparison of the yield from ring opening of butyl glycidyl ether with that from *tert*-butyl glycidyl ether, the yield of **8** and **9** was obtained similarly to **6** and **7** at 70°C for 10 min. Thus, the alkyl group of ether could not affect to ring opening reaction of alkyl glycidyl ether. In addition, the ether linkage was not reactive in this reaction. Four isomeric products were separated by silica gel column chromatography and characterized by ¹H-NMR spectroscopy.

The ¹H-NMR spectrum of 3-butoxy-2-methoxypropan-1-ol (**6**) exhibited the signal of $-\text{CHOCH}_3$ as a multiplet (1H) at δ 3.87-3.91, $-\text{OCH}_2\text{CHOCH}_3$ as a multiplet (2H) at δ 3.45-3.51, $-\text{OCH}_2\text{CH}_2$ and $-\text{CH}_2\text{OH}$ as a multiplet (4H) at δ 3.55-3.61, $-\text{OCH}_3$ as a singlet (3H) at δ 3.41, $-\text{OCH}_2\text{CH}_2$ as a multiplet (2H) at δ 1.38-1.48, $-\text{CH}_2\text{CH}_2\text{CH}_3$ as a multiplet (2H) at δ 1.17-1.30 and $-\text{CH}_3$ as a triplet (3H) at δ 0.86 ($J = 7.3$ Hz)

The ¹H-NMR spectrum of 1-butoxy-3-methoxypropan-2-ol (**7**) exhibited the signal of $-\text{CHOH}$ as a triplet (1H) at δ 4.90 ($J = 3.6$ Hz), $-\text{CH}_2\text{OBu}$ and $-\text{CH}_2\text{OCH}_3$ as a multiplet (4H) at δ 3.69-3.72, $-\text{OCH}_2\text{CH}_2$ as a triplet (1H) at δ 3.49 ($J = 3.6$ Hz), $-\text{OCH}_3$ as a singlet (3H) at δ 3.24, $-\text{OCH}_2\text{CH}_2$ as a quintet (2H) at δ 1.46 ($J = 7.0$

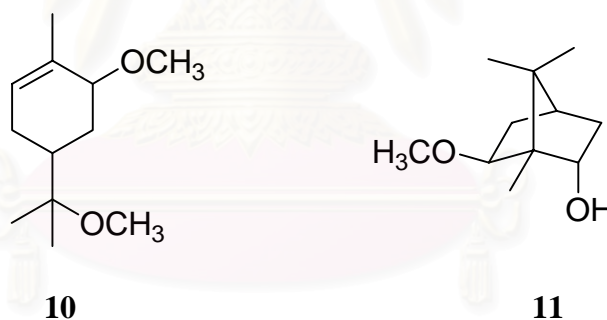
Hz), $-\text{CH}_2\text{CH}_2\text{CH}_3$ as a multiplet (2H) at δ 1.33 ($J = 7.0$ Hz) and $-\text{CH}_3$ as a triplet at δ 0.96 ($J = 7.3$ Hz).

The $^1\text{H-NMR}$ spectrum of 3-*tert*-butoxy-2-methoxy-propan-1-ol (**8**) exhibited the $-\text{CHOCH}_3$ as a singlet (1H) at δ 3.80, $-\text{CH}_2\text{OH}$ as a multiplet (4H) at δ 3.31-3.50, $-\text{OCH}_3$ as a singlet (3H) at δ 3.39 and $-\text{C}(\text{CH}_3)_3$ as a singlet (9H) at δ 1.20

The $^1\text{H-NMR}$ spectrum of 1-*tert*-butoxy-3-methoxy-propan-2-ol (**9**) revealed the $-\text{CHOH}$ signal as a triplet (1H) at δ 4.90 ($J = 3.6$ Hz), $-\text{CH}_2\text{OCH}_3$ as a multiplet (4H) at δ 3.69-3.75, $-\text{OCH}_3$ as a singlet (3H) at δ 3.24 and $-\text{C}(\text{CH}_3)_3$ as a singlet (9H) at δ 1.21.

4.5.8.4 Ring opening of α -pinene oxide

α -Pinene oxide was chosen as a representative of bicyclic epoxide. The ring opening reaction of α -pinene oxide with MeOH at 70°C for 10 min furnished two major products, **10** (49.39%) and **11** (29.36%).



The ring opening of α -pinene oxide could be successfully performed using Fe-pillared bentonite, two major products obtained were characterized as sobrerol dimethyl ether (**10**) and 6-methoxy-1,7,7-trimethyl-bicyclo[2.2.1]heptan-2-ol (**11**) [42]. The reaction gave the desired products in moderate yield.

The products from this reaction were separated by silica gel column chromatography yielding two major products. The structures of these two products were characterized by $^1\text{H-NMR}$. To illustrate this, **10** exhibited the peaks of $-\text{CH}=\text{CCH}_3$ as a multiplet (1H) at δ 5.56-5.60, the peaks of $-\text{CHOCH}_3$ as a multiplet (1H) at 3.50. The peak of $-\text{CHOCH}_3$ as a singlet (3H) at δ 3.39 and the peak of $-\text{C}(\text{CH}_3)_3\text{OCH}_3$ as a singlet (3H) at δ 3.17. The peak of $-\text{CH}_2\text{CH}=\text{CCH}_3$ as a double

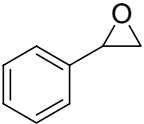
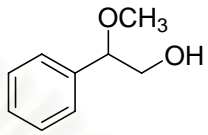
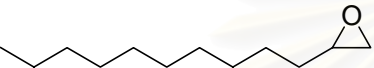
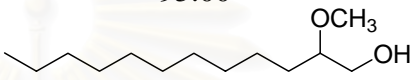
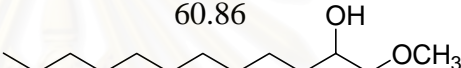
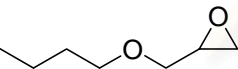
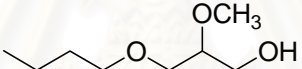
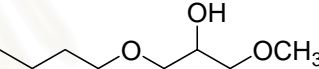
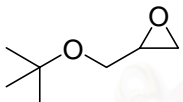
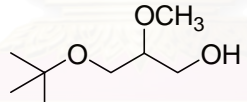
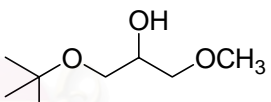
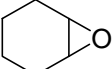
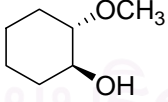

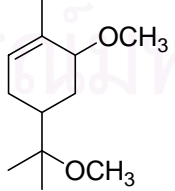
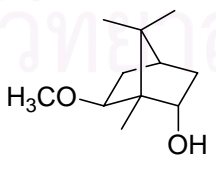
doublet (2H) at δ 2.12 ($J = 1.8, 13.6$ Hz), those of $-\text{CH}_2\text{CHCH}_3$ as a multiplet (2H) at 1.98-2.03 and $-\text{CHC}(\text{CH}_3)_3\text{OCH}_3$ as a multiplet (1H) 1.92-1.98. The peak of $-\text{CH}=\text{CCH}_3$ as a singlet (3H) at δ 1.76 and the two peaks of $-\text{CHC}(\text{CH}_3)_2$ both as a singlet (6H) at δ 1.11 and 1.10.

The structures of the other product, 6-methoxy-1,7,7-trimethyl-bicyclo[2.2.1] heptan-2-ol (**11**), was fully characterized by $^1\text{H-NMR}$. To illustrate this, the peak of $-\text{CHOH}$ was detected as a singlet (1H) at δ 4.03 and $-\text{CHOCH}_3$ as a double doublet (1H) at δ 3.85 ($J = 3.0, 9.6$ Hz). The peak of $-\text{OCH}_3$ as a singlet (3H) at δ 3.35. The peak of $-\text{CH}_2\text{CHOH}$ as a multiplet (2H) at δ 2.27-2.38 and those of $-\text{CHC}(\text{CH}_3)_2$ as a multiplet (1H) at δ 1.56-1.66. The two peaks of $-\text{CH}_2\text{OCH}_3$ was shown as a double doublet (1H) at δ 1.35 ($J = 3.0, 13.0$ Hz) and as a multiplet (1H) at δ 1.22-1.29. The peak of $-\text{CCH}_3$ as a singlet (3H) at δ 1.06, those of $-\text{C}(\text{CH}_3)_2$ as a singlet (3H) at δ 0.84 and a singlet (3H) at δ 0.83.

4.5.9 Summary of epoxide ring opening catalyzed by Fe-pillared bentonite

Various epoxides (styrene oxide, 1-dodecene oxide, cyclohexene oxide, butyl glycidyl ether, *tert*-butyl glycidyl ether and α -pinene oxide) were selected to perform ring opening with MeOH catalyzed by Fe-pillared bentonite under standard conditions (70°C for 10 min). The results are summarized in Table 4.16.

Table 4.16 Ring opening of various epoxides with MeOH catalyzed by Fe-pillared bentonite

Entry	Epoxide	% yield of product (based on substrate)	selectivity
1		 95.00	-
2		 60.86  40.15	1.52
3		 52.64  21.83	2.41
4		 57.06  14.09	4.05
5		 83.07	-
6		 49.39  29.36	

Reaction conditions: epoxide (1 mmol), MeOH (3 mL), 30 wt% Fe-pillared bentonite to styrene oxide at 70°C for 10 min.

Table 4.16 shows that Fe-pillared bentonite can act as an efficient catalyst for epoxide ring opening with MeOH as a nucleophile at 70°C for 10 min. Entry 1 shows that the reaction of aromatic epoxide, styrene oxide underwent the cleavage with MeOH with preferential attack at the benzylic position. Only a single product was obtained in quantitative yield. Entries 2-4 reveal that the reaction of aliphatic epoxide as 1-dodecene oxide, epoxides containing ether functional group as butyl glycidyl ether and *tert*-butyl glycidyl ether could also be accomplished and furnished the desired products in high to excellent yield. In the case of unsymmetrical epoxides, the regioselectivity clearly pointed out that it was strongly depended on the nature of the substituent. Entry 5 shows that the reaction of cyclic epoxide as cyclohexene oxide was completed antisteroselective and *trans* products were obtained in quantitative yield. Entry 6 exhibited that bicyclic epoxide as α -pinene oxide could be transformed into two major products. The reaction gave the desired products in good yield.



สถาบันวิทยบริการ
จุฬาลงกรณ์มหาวิทยาลัย

CHAPTER V

CONCLUSION

From the preceding results and discussion, the main focus of this research is to search for the optimum conditions for the ring opening of epoxides catalyzed by Fe-pillared clays.

Fe-pillared hectorite and bentonite were synthesized by the intercalation of iron complexes into clay interlayers and calcination at 300⁰C for 5 h. All synthesized products were characterized using XRD, N₂ adsorption-desorption, redox titration and base titration. The XRD patterns of the Fe-pillared clays indicate that the layered structure of clay is sustained. The d₀₀₁ spacing of Fe-pillared hectorite and Fe-pillared bentonite are reported for 10.37 Å and 9.65 Å, respectively. The nitrogen adsorption-desorption isotherms of Fe-pillared clays suggested the distorted reversible type IV isotherm indicating that Fe₂O₃ in calcined samples converting clay-layered structure to mesoporous structure. Therefore, the BET specific surface areas of Fe-pillared clays are higher than those of pure clays. From the results of titration, iron contents and acidity of Fe-pillared clays are higher than pure clays. Fe-pillared bentonite exhibited the highest iron content (29.18% Fe₂O₃ form) and the highest acidity (150.15 meq/100 g of clay).

The Fe-pillared clays are then used for ring opening reaction. Styrene oxide is the model employed using MeOH as a nucleophile. The optimum condition for styrene oxide ring opening with MeOH is 30 wt% Fe-pillared bentonite to styrene oxide at 70⁰C for 10 min. The reaction could be performed to furnish 2-methoxy-2-phenylethanol in quantitative yield with excellent selectivity. Under the same reaction condition, Fe-pillared bentonite shows better efficiency than Fe-pillared hectorite because Fe-pillared bentonite has higher acidity than Fe-pillared hectorite.

The ring opening study is also applied to other epoxides, such as 1-dodecene oxide, butyl glycidyl ether, *tert*-butyl glycidyl ether, cyclohexene oxide and α -pinene

oxide. Two regioisomers were obtained from the ring opening of 1-dodecene oxide, butyl glycidyl ether and *tert*-butyl glycidyl ether with moderate yields. While cyclohexene oxide ring opening achieved the desired product in quantitative yield. The ring opening of α -pinene oxide yielded two major products.

The mechanism of epoxide ring opening reaction catalyzed by Fe-pillared clay is confirmed to occur *via* S_N-1 reaction. This catalyst is first coordinated with an oxygen atom of epoxide to induce partial charge species. Then a nucleophile could attack the epoxide ring at that site to furnish the desired products.

Propose for the future work

This research focuses on the methodology of epoxide ring opening reaction with Fe-pillared clay catalyst. Other metals such as Al and Ni/Al may be used instead of iron in pillared clay catalyst to improve percentage yield and selectivity of the reaction. The Al complexes are commonly used to pillar the clay structure, since they are large and relatively stable. The aluminium oxide-pillared clays usually have large d-spacing between clay layers and high surface area. Nikle can be doped onto aluminium oxide-pillared clays to modify its acidity, selectivity of this reaction. Other epoxides and nucleophiles can be tested to expand the scope of the reaction.

สถาบันวิทยบริการ
จุฬาลงกรณ์มหาวิทยาลัย

REFERENCES

1. Baltork, I. M.; Tangestaninejad, S.; Aliyan H.; Mirkhani, V. Bismuth(III) chloride (BiCl_3); an efficient catalyst for mild, regio- and stereoselective cleavage of epoxides with alcohols, acetic acid and water. *Synth. Comm.*, **2000**, *30(13)*, 2365.
2. Ha, J. D.; Kim, S. Y.; Lee, S. J.; Kang, S. K.; Ahn, J. H.; Kim, S. S.; Choi, J. K. Regio- and stereoselective ring opening of vinyl epoxides with MgBr_2 . *Tetrahedron Lett.*, **2004**, *45*, 5969.
3. Sharghi, H.; Nasserri, M. A.; Najad, A. H. Efficient synthesis of β -hydroxy thiocyanates from epoxides and ammonium thiocyanates using tetraarylporphyrins as new catalysts. *J. Mol. Catal. A*, in press
4. Chini, M.; Crotti, P.; Macchia, F. Metal salts as new catalysts for mild and efficient aminolysis of oxiranes *Tetrahedron Lett*, **1990**, *31*, 4661.
5. Yadav, J. S.; Reddy, B. V. S.; Reddy, C. S. SelectfluorTM: a novel and efficient reagent for the synthesis of β -hydroxy thiocyanates. *Tetrahedron Lett.*, **2004**, *45*, 1291.
6. Yadav, J. S.; Reddy, B. V. S.; Dasak, A. K.; Narsaiah, A. V. [Bmim] BF_4 ionic liquid: a novel reaction medium for the synthesis of β -amino alcohols. *Tetrahedron Lett.*, **2003**, *44*, 1047.
7. Xu, L. W.; Li, L.; Xia, C. G.; Zhao, P. Q. Efficient synthesis of chlorohydrins: ionic liquid promoted ring-opening reaction of epoxides and TMSCl . *Tetrahedron Lett.*, **2004**, *45*, 2435.
8. Taniguchi, Y.; Tanaka, S.; Kitamura, T.; Fujiwara, Y. Lanthanoid-catalyzed ring-opening reaction of epoxides with acyl Halides. *Tetrahedron Lett.*, **1998**, *39*, 4559.
9. Mizuno, M.; Shioiri, T. Ring opening reaction of epoxides with diphenyl phosphorazidate. *Tetrahedron Lett.*, **1999**, *40*, 7105.
10. Ollevier, T.; Lavie-Compin, G. An efficient method for the ring opening of epoxides with aromatic amines catalyzed by bismuth trichloride. *Tetrahedron Lett.*, **2002**, *43*, 7891.

11. Moghadam, M.; Tangestaninejad, S.; Mirkhani, V.; Shaibani, R. Rapid and efficient ring opening of epoxides catalyzed by a new electron deficient tin(IV) porphyrin. *Tetrahedron*, **2004**, *60*, 6105.
12. Uyanik, C.; Hanson, J.R.; Hitchcock, P. B.; Lazar, M. A. Steric effects in the tetracyanoethylene catalysed methanolysis of some cyclohexane epoxides. *Tetrahedron*, **2005**, *61*, 4323.
13. Yadav, J. S.; Reddy, B. V. S.; Jyothirmai, B.; Murty, M. S. R. Ionic liquids/H₂O systems for the reaction of epoxides with NaN₃: a new protocol for the synthesis of 2-azidoalcohols. *Tetrahedron Lett.*, **2005**, *46*, 6559.
14. Posner, G. H.; Rogers, D. Z.; Kinzig, C. M.; Gurria, G. M. Organic reactions at alumina surfaces. Displacement reactions effected by alcohols, thiols, and acetic acid on dehydrated alumina. *Tetrahedron Lett.*, **1975**, *16*, 3597.
15. Otera, J.; Yoshinaga, Y.; Hirakawa, K. Highly regioselective ring opening of epoxides with alcohols catalyzed by organotin phosphate condensates. *Tetrahedron Lett.*, **1985**, *26*, 3219.
16. Choudary, B. M.; Sudha, Y. Fe³⁺-montmorillonite: an efficient heterogeneous catalyst for highly regioselective alcoholysis of epoxides. *Synth. Comm.*, **1996**, *26(16)*, 2989.
17. Iranpoor, N.; Zardaloo, F. S. Tris[trinitrato Ce(IV) parareriolate], an efficient heterogeneous catalyst for alcoholysis, acetolysis and hydrolysis of epoxides. *Synth. Comm.*, **1994**, *24(14)*, 1959.
18. Iranpoor, N.; Tarran, T.; Movahedi, Z. FeCl₃.6H₂O supported on SiO₂ catalysed ring opening of epoxides with alcohols, acetic acid, water, chloride, bromide and nitrate ions. *Synthesis.*, **1996**, 1473.
19. Kantam, M. L.; Santhi, P. L.; Prasad, K. V.; Figueras, F. Iron pillared clay-an efficient catalyst for ring opening of oxiranes. *J. Mol. Catal.*, **2000**, 289.
20. Ishich, S.; Suzuki, S.; Hayano, T.; Furuno, H.; Inanaga, J. Heterogeneous catalysis of novel polymeric rare earth complexes under solvent-free conditions: Zero-emission synthesis of β-amino alcohols. *J. Alloys Compound*, **2005**, *408-412*, 441.

21. Bart, M. L.; Jacobs, P. A. Impregnation of dimeric Cr^{III} (salen) on silica and its application in epoxide asymmetric ring opening reactions. *Appl. Catal. A*, **2005**, 282, 181.
22. Nagendrappa, G. Organic synthesis using clay catalysts. *Resonance*, **2002**, 64.
23. Varma, R. S. Clay and clay-supported reagents in organic synthesis. *Tetrahedron*, **2002**, 58, 1235.
24. Bruce, W. D.; O'Hare, D. Inorganic material, 2nd ed., New York, John Wiley & Sons, Inc., **1997**.
25. Shichi, T.; Takagi, K. Clay minerals as photochemical reaction fields. *Journal of Photochemistry and Photobiology C: Photochemistry Reviews I*, **2000**, 113.
26. Moore, D. M.; Reynolds, Jr. R. C. X-Ray Diffraction and the Identification and Analysis of Clay Minerals, New York, USA, Oxford University Press, **1989**.
27. Michael, R.; Grace, S. T.; Vishnu, K. The many ways of making anionic clays *Proc. Indian Acad. Sci. (Chem. Sci.)*, **2001**, 113, 671.
28. Jean, F. L.; Georges, P. Acidity in pillared clays: origin and catalytic manifestations. *Topic in Catalysis 4*, **1997**, 43.
29. Robert, A. S.; Tom, P.; Gerhard, L.; Nick, G. Pillared clays and pillared layered solids (technical report). *Pure Appl. Chem.*, **1999**, 71, 2367.
30. Vicente, M. A.; Belver, C.; Trujillano, R.; Banares-Munoz, M. A.; Rives, V.; Korili, S. A.; Gil, A.; Gandia, L. M.; Lambert, J. F. Preparation and characterisation of vanadium catalysts supported over alumina-pillared clays. *Catalysis Today* **2003**, 78, 181.
31. Gonzalez, F.; Pesquera, C.; Blanco, C.; Benito, I.; Mendioroz, S. Synthesis and characterization of Al-Ga pillared clays with high thermal and hydrothermal stability. *Inorg. Chem.*, **1992**, 31, 727.
32. Basic operating principles of the sorptomatic 1990. Available from: <http://saf.chem.ox.ac.uk/Instruments/BET/sorpoptprin>.
33. Analysis software user's manual, BELSORP, BEL JAPAN, INC. 57.
34. Gilbert, H. A.; Quantitative Chemical analysis, New York, USA, Harper & Row, 1968

35. Solomon G. T. W. Fundamentals of organic chemistry, 5th ed., New York, John Wiley & Sons, Inc., **1997**.
36. Loudou, G. M. Organic chemistry, 3rd ed., The Benjamin/Cummings publishing company, Inc., 1995
37. Kanjanaboonmalert, T. Synthesis and catalytic activity in alkylation reaction of iron and gallium-dopes iron oxides pillared clays. Master's Thesis, Department of Chemistry, Faculty of Science, Chulalongkorn University, 2004.
38. Klurvudtikul, P. Adsorption of olefins in BTX feedstock. Master's Thesis, Program of Petrochemistry and Polymer Science, Faculty of Science, Chulalongkorn University, 2002.
39. Jetipattaranat, W. Epoxides ring opening reaction utilizing transition metal catalysts. Master's Thesis, Program of Petrochemistry and Polymer Science, Faculty of Science, Chulalongkorn University, 2003.
40. Winstein, S.; Ingraham, L. L. Neighboring carbon and hydrogen. XVII. The pinacol rearrangement. Solvolysis of 2-methoxy-2-phenylethanol and related halides. *J. Am. Chem. Soc.*, **1955**, 77, 1738.
41. Iranpoor, N.; Adibi, H. Iron(III) trifluoroacetate as an efficient catalyst for solvolytic and nonsolvolytic nucleophilic ring opening of epoxides. *Bull. Chem. Soc. Jpn.*, **2000**, 73, 675
42. Motherwell, W. B.; Bingham, M. J.; Six, Y. A study of some molecularly imprinted polymers as protic catalysts for the isomerisation of α -pinene oxide to *trans*-carveol. *Tetrahedron*, **2004**, 60, 3231.



Appendices

สถาบันวิทยบริการ
จุฬาลงกรณ์มหาวิทยาลัย

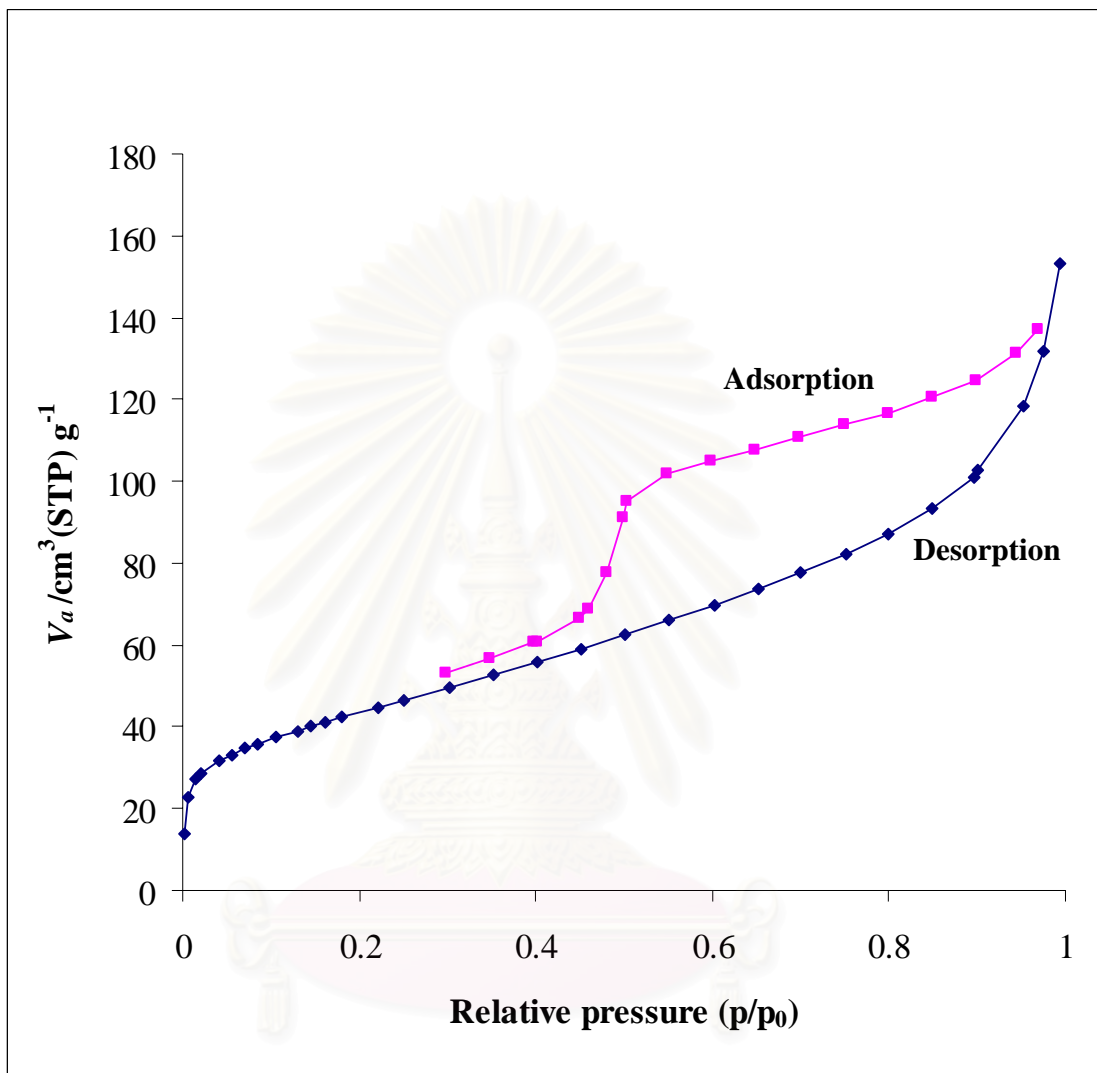


Figure A-1 N_2 adsorption-desorption isotherm of Fe-pillared bentonite (BFe₁₀).

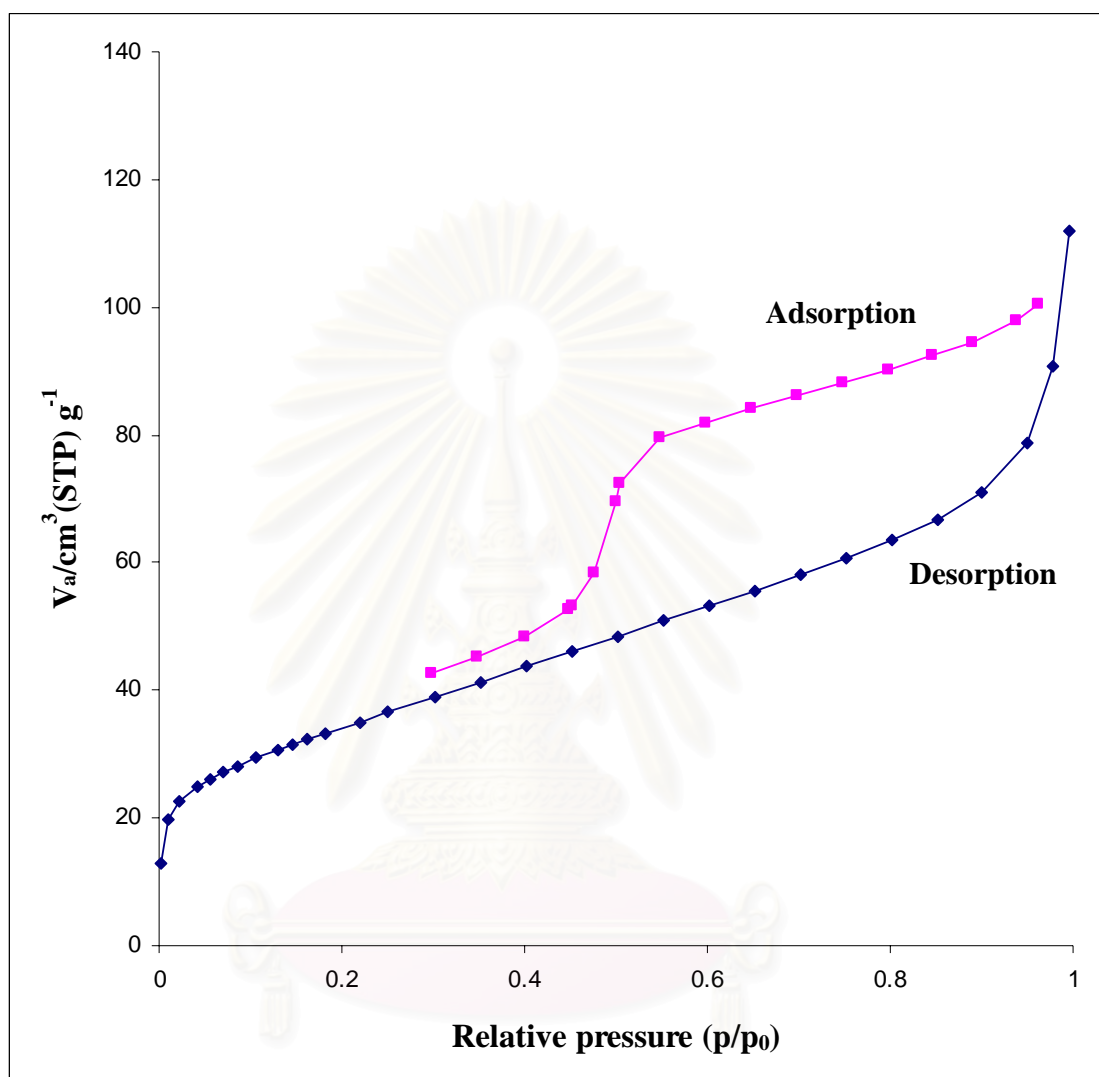
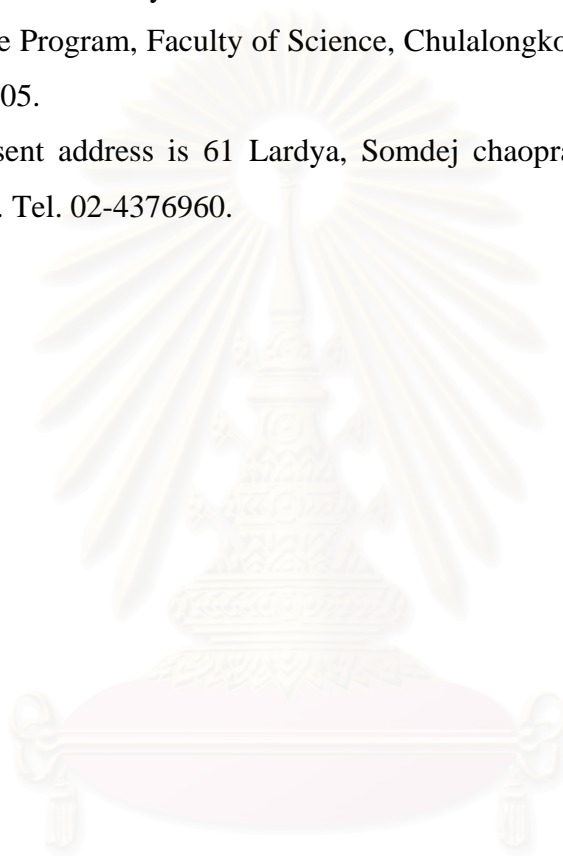


Figure A-2 N_2 adsorption-desorption isotherm of Fe-pillared hectorite (HFe_{10}).

VITA

Miss Piyarat Trikittiwong was born on January 17, 1982 in Bangkok, Thailand. She graduated with Bachelor's Degree in Chemistry from Faculty of Science, Mahidol University in 2004. She continued her study in Petrochemistry and Polymer Science Program, Faculty of Science, Chulalongkorn University in 2004 and completed in 2005.

Her present address is 61 Lardya, Somdej chaopraya, Khongsan, Bangkok, Thailand 10600. Tel. 02-4376960.



สถาบันวิทยบริการ
จุฬาลงกรณ์มหาวิทยาลัย